



Technological University Dublin
ARROW@TU Dublin

Masters

Science

2010-01-01

Mig-6 and Its Role in Regulating Adult Lung Epithelium

Sandra Bennett

Technological University Dublin

Follow this and additional works at: <https://arrow.tudublin.ie/scienmas>

Recommended Citation

Bennett, S. (2010). *Mig-6 and Its Role in Regulating Adult Lung Epithelium*. Masters dissertation. Technological University Dublin. doi:10.21427/D78P5G

This Theses, Masters is brought to you for free and open access by the Science at ARROW@TU Dublin. It has been accepted for inclusion in Masters by an authorized administrator of ARROW@TU Dublin. For more information, please contact yvonne.desmond@tudublin.ie, arrow.admin@tudublin.ie, brian.widdis@tudublin.ie.



This work is licensed under a [Creative Commons Attribution-Noncommercial-Share Alike 3.0 License](https://creativecommons.org/licenses/by-nc-sa/3.0/)





Mig-6 and its role in regulating Adult Lung Epithelium

A thesis submitted to the Dublin Institute of Technology in fulfilment of the requirements for award of Masters (MPhil) in Biomedical Sciences

School of Biological Sciences,
Dublin Institute of Technology,
Kevin St, Dublin 8

In conjunction with FAS Science Challenge,
Baylor College of Medicine,
Houston, Texas, U.S.A.



Sandra Bennett

October 2010

Table of Contents	Page
Acknowledgements	5
Abbreviations	6
1.0 Introduction	9
1.1 The Lung	10
1.2 Mouse Models for lung cancer	17
1.3 Cell Signalling	21
1.4 Mig-6	30
Aims	36
2.0 Materials and Methods	
2.1 siRNA treatment of epithelial and endothelial cells	37
2.2 EGF/HGF induction of Mig-6 in siRNA treated cells	39
2.3 SDS PAGE and Western blot	40
2.4 RNA Isolation	46
2.5 Quantitative Real Time PCR	48
2.6 Measurement of Alveolar Spaces	50
2.7 MTT Assay	51
2.8 Analysis of H441 cell line for mutated <i>Mig-6</i>	53
2.8.1 <i>Mig-6</i> PCR	55
2.8.2 DNA Purification from agarose gel	56
2.8.3 TOPO[®] Cloning Reaction	57
2.8.4 Analysis of positive clones	57
2.8.5 Plasmid Isolation and DNA purification	58
2.8.6 EcoRI digestion of plasmid	58
2.8.7	

3.0 Results

3.1 Real time PCR to show knock-out of Mig-6 in Mig-6 ^{-/-} mice and induced knock-out of Mig-6 in Tamoxifen treated Cre ⁺ d/d mice	60
3.2 Comparison of the morphology of Mig-6 ^{f/f} and Mig-6 ^{d/d} adult mouse lungs	
3.3 Adult Mig-6 ^{f/f} and Mig-6 ^{d/d} mice have normal alveolar spaces	62
3.4 Expression of Pulmonary Epithelial Cell markers in Mig-6 ^{-/-} vs. Mig-6 ^{+/+}	
3.4.1 CCSP levels	65
3.4.2 T1 Alpha levels	66
3.4.3 SP-C levels	68
3.4.4 MUC5AC levels	69
3.5 Silencing of Mig-6 expression in H441 epithelial lung cells using RNA interference	71
3.6 Silencing Mig-6 expression in HMVEC endothelial lung cells using RNA interference	73
3.7 Knockdown of Mig-6 leads to changes in cell proliferation: MTT assay	75
3.8 Analysis of H441 cell line for mutated <i>Mig-6</i>	77
3.9 Western blot analysis of siRNA treated and untreated cells	79
3.9.1 HGF Induction of Mig-6 in H441 and NHBE cells	80
3.9.2 EGF Induction of Mig-6 in H441 and NHBE cells	83
3.9.3 p-Akt levels in H441 cells in the presence and absence of EGF	86
4.0 Discussion	90
References	99

Declaration

I hereby certify that the material which is submitted in this thesis towards award of **MPhil in Biomedical Sciences** is entirely my own work and has not been submitted for any academic assessment other than for the fulfilment of the award named above.

Signature of candidate:

Date:

Acknowledgements

Firstly I would like to thank Dr. Franco DeMayo at Baylor College of Medicine for allowing me to be a project intern in his laboratory.

In particular I would like to thank Nili Jin for all of her help and guidance whilst carrying out this work alongside her.

Thanks also to the staff in the molecular cell biology department at Baylor College of Medicine, especially those in the DeMayo laboratory.

Thanks to my supervisors at DIT, Dr. James Curtin and Dr. Fergus Ryan for all of their help and advice in putting together this thesis.

Finally I would like to acknowledge my friends and family for all of their support and encouragement.

Abbreviations

BEBM	Bronchial Epithelial Cell Basal Medium
BPD	BronchoPulmonary Dysplasia
CCSP	Clara Cell Secretory Protein
COPD	Chronic Obstructive Pulmonary Disease
CRIB domain	Cdc42/Rac interaction and binding domain
DEPC	Diethylpyrocarbonate
EGF	Epidermal Growth Factor
EGFR	Epidermal Growth Factor Receptor
ES cells	Embryonic Stem Cells
FBS	Foetal Bovine Serum
FGF	Fibroblast Growth Factor
HGF	Hepatocyte Growth Factor
LoxP	locus of X over in PI
Mig-6	Mitogen inducible gene 6
Mig-6^{-/-} mice	Mig-6 knockout mice
Mig-6^{dl/d} mice	<i>Rosa26-Cre-ERT2</i> x <i>Mig-6flox/flox</i> mice
Mig-6^{ff} mice	<i>Mig-6flox/flox</i> mice

NHBE	Normal Human Bronchial Epithelial cells
PBS	Phosphate Buffered Saline
PCR	Polymerase Chain Reaction
PDGF	Platelet Derived Growth Factor
PTB domain	Phosphotyrosine-Binding domain
RALT	Receptor Associated Late Transducer
RTK	Receptor Tyrosine Kinase
SH2 domain	Src-homology-2 (SH2) domain
SH3 domain	Src-homology 3 domain
SOCS	Suppressor of Cytokine Signalling
SP-C	Surfactant Protein C
SSRs	Site specific recombinases
TBS	Tris Buffered Saline
TBST	Tris Buffered Saline & Tween
TGFα	Tumour Growth Factor alpha
TK	Tyrosine Kinase
TTF-1	Thyroid Specific Transcription Factor

Abstract

Through the use of developmental and knock out studies Mig-6 has been shown to have a role in development. It has also been shown to be a tumour suppressor gene. Little work has been done as yet looking at its role in the adult.

This study examined the role of Mig-6 in the lung with the ultimate goal being to determine if the pulmonary phenotype due to Mig-6 ablation is due to a developmental programming or loss of function in the adult. This was investigated in two ways.

1. To investigate if knocking out Mig-6 in adult lung has an effect on lung function
2. Investigate the role of Mig-6 in lung epithelial cells by RNAi (Investigation of the Role of Mig-6 in Pulmonary Epithelial Cells and Vascular Cells *In Vitro*).

Knocking out Mig-6 in the adult mice showed no difference in epithelial markers and after staining morphology and airway size were found to be normal. This would seem to indicate that the Mig-6 phenotype is due to altered development of the lungs during the neonatal period and not due to a loss of function in the adult.

From the cell work we observed differences in the effect on epithelial cells vs. endothelial cells when Mig-6 was knocked out. The epithelial cells showed an increased number of viable cells present after knocking out Mig-6 while the number of viable cells was decreased in the endothelial cells. This would indicate that knocking out Mig-6 in epithelial cells causes increased proliferation but in endothelial cells causes apoptosis.

Conclusions: Ablation of Mig-6 leads to increased proliferation in epithelial cells (and apoptosis in endothelial cells) but knocking it out in the adult stage has a mild effect on lung phenotype

1. Introduction

Mig-6 is an immediate early response gene which is transcriptionally induced by a number of factors including growth factors, stress, cytokines and the Ras oncoprotein (1,2,3). This gene is only present in higher eukaryotes (4) and can be rapidly induced allowing it to potentially be involved in early regulation of cellular responses (4). Mig-6 has been shown to be involved in the EGF signalling pathway (4) and has been proposed to be involved in the HGF signalling pathway as a negative regulator. It has previously been shown in our laboratory that Mig-6 levels in the lung change throughout development and that Mig-6 has a developmental role (5) so the overall aim of our work was to investigate whether Mig-6 also played a role post-natally.

A Mig-6 knockout mouse (Mig-6^{-/-}) has been developed by the DeMayo lab at Baylor College of Medicine where Mig-6 has been knocked out at the germline level which has enabled us to look at what occurs during development in the absence of Mig-6 (6). The embryo lethal phenotype and multi-tissue carcinogenesis of the Mig-6 null allele make it difficult to investigate the impact of ablation of Mig-6 on specific tissues and at specific time points during development. A conditional knockout would overcome this.

Our lab developed an inducible ablation model by crossing *Rosa26-Cre-ERT2* mice with Mig-6^{flox/flox} mice providing us with a population of Cre positive mice in addition to Cre negative mice. Administration of Tamoxifen to Cre positive mice would induce ablation of Mig-6 and allow us to look at what effects (if any) this would have on adult mice.

1.1 The Lung

Lung Function

The lung is a complex organ composed of more than 40 different cell types whose main function is in gaseous exchange (7, 8, 9, 10, 11). The various cell types are heterogeneously distributed within a highly complex framework of branching that eventually terminates with the alveoli. Gaseous exchange occurs across the thin epithelium of the millions of alveoli which have a surface area of approx. 100m^2 which is sufficient to carry out gas exchange for the entire body, which is important as every single cell in the body needs a constant supply of oxygen in order to produce enough energy to grow, repair or replace itself and to maintain vital functions (12). The pulmonary epithelium has a number of functions other than gaseous exchange. It provides a protective barrier between the host and the outside environment by segregating inhaled foreign agents, and it also controls the movement of solutes and water, contributing to the maintenance of lung fluid balance (13). Lung epithelium plays a role in the metabolism of endogenous mediators and is capable of regeneration, allowing normal cell turnover and restoration of airway and alveolar functions after lung injury. Lung epithelium produces surfactant and several proteins which are important as part of the immune defences of the body (14).

Lung Structure:

The respiratory system (shown in figure 1.1) can be divided into upper and lower. The upper respiratory system is comprised of the nasal cavity, paranasal sinuses and the nasopharynx. The lower respiratory tract begins at the larynx followed by the trachea which divides to form the right and left primary bronchi each of which divides to form secondary (lobar) bronchi and then tertiary (segmental) bronchi. Tertiary bronchi divide into numerous bronchioles. The terminal bronchioles divide into the respiratory bronchioles, alveolar ducts and alveolar sacs

which open into the alveoli. The respiratory epithelium undergoes progressive transition from tall, pseudostratified columnar, ciliated form in the larynx and trachea to a simple, cuboidal non-ciliated form in the alveoli .

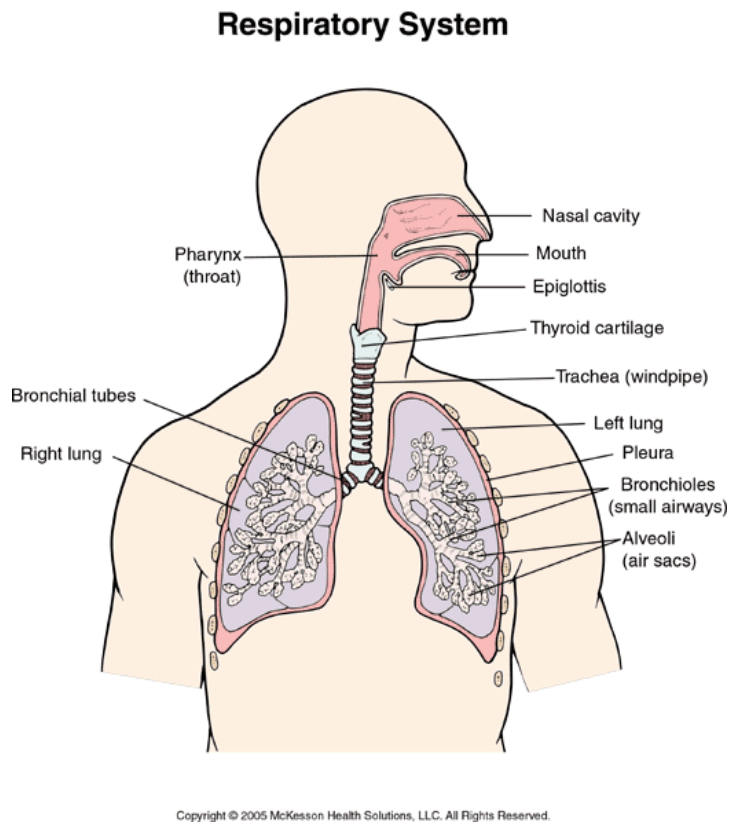


Figure 1.1: diagram illustrating the overall structure of the respiratory system (15)

It is the alveoli which perform the function of gaseous exchange. The alveolar wall is made up of epithelial cells, supporting tissues and blood vessels. The epithelial layer consists of type I and type II pneumocytes. Type I pneumocytes are part of the gaseous diffusion barrier while the type II pneumocytes secrete surfactant which serves to reduce surface tension in the alveoli and prevents alveolar collapse during expiration .

Lung Development:

In mammals most of the structural development and maturation of the lung takes place *in utero* (16). In humans, there are four stages of pre-natal lung development (shown in Figure 1.2):

1. Embryonic (up to 7 weeks gestation)
2. Pseudoglandular (5-17 weeks of gestation)
3. Canalicular (16-27 weeks of gestation)
4. Alveolar (27 weeks gestation to term)

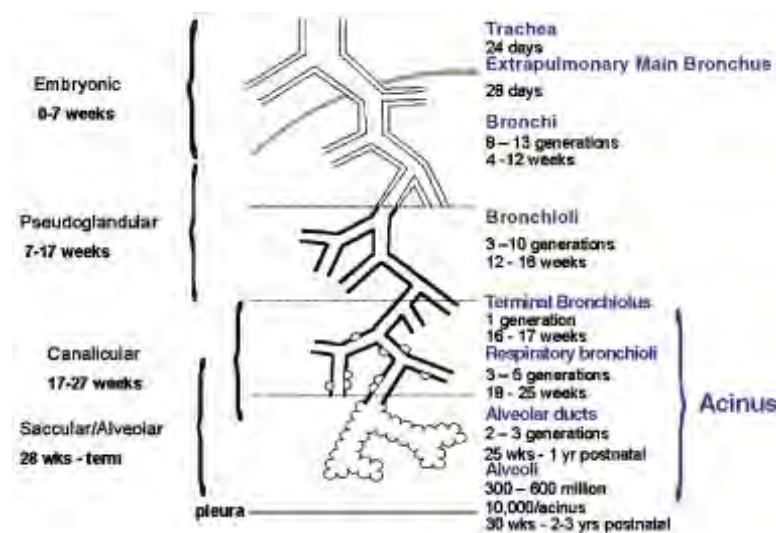


Figure 1.2: diagram of lung development showing the time points at which different structures appear (16).

During the pseudo glandular phase of lung development, major development events occur in which the airway wall cells differentiate into cartilage, sub mucosal gland, bronchial smooth muscle and epithelial cell types. The epithelium differentiates into type I and type II pneumocytes during the canalicular stage.

The blood vessel network develops at the same time as the airways. At 28 days gestation, groups of endothelial cells can be found in the mesenchyme. At 34 days, capillaries lined by

endothelial cells surround the two primitive lung buds. As branching of the developing airways proceeds, each new bud is surrounded by a halo of endothelial cells (16).

Molecular Regulation of Lung Development:

Genetic factors are critical to early lung morphogenesis and post natal maturation. Alteration of any of the essential genes disturbs the regulation of development and results in neonatal lung disease and abnormally developed lungs. Abnormally developed lungs have a higher propensity towards lung disease such as chronic obstructive pulmonary disease (COPD) and asthma. Growth factors mediate tissue interactions and regulate a variety of cellular functions that are critical for normal lung development and homeostasis (17). Epidermal growth factor (EGF) members have been implicated in the development and maturation of the respiratory system in a diverse range of animal species. It has been found that mice deficient in EGF receptor (EGFR) show delayed lung maturation which is characterised by poor alveolarisation and abnormal branching. Decreased alveolarisation and septation in these mice correlates with low expression of surfactant protein C (SP-C) and thyroid specific transcription factor (TTF-1) (11). EGF and EGFR are increased in lungs with BronchoPulmonary Dysplasia (BPD) and fibrosis. Over-expression of the EGFR ligand and tumour growth factor alpha (TGF α) in perinatal lungs causes disrupted alveolarisation and vascularisation which leads to fibrosis in adulthood.

Among the essential factors that regulate lung development, EGF signalling is important for both early stage and late- stage lung development. Ablation of EGFR leads to reduced lung branching and changed epithelial cells.

Lung Disease:

Lung disease is classed as any disorder where lung function is impaired (18). Lung disease is the number three killer (behind heart disease and cancer) in the USA and is responsible for one in six deaths. Deaths due to heart disease are falling while in contrast, deaths due to lung disease are increasing each year (19). Lung disease can occur as a result of a number of different factors such as exposure to tobacco smoke (both actively and passively), air pollutants, occupational exposure to foreign particles such as silica dust or asbestos, carcinogens, infectious agents and overactive immune system defences (18). In many cases there is not just one single cause that can be attributed to the lung disease present, often the disorder is caused by a number of the factors outlined above. Diseases which affect the respiratory system include: obstructive lung diseases like asthma and emphysema, respiratory distress syndrome, pulmonary oedema, pulmonary fibrosis and lung cancer. Infectious agents affecting the lung include respiratory syncytial virus (RSV), TB, influenza as well as other bacteria and viruses (18). Genetic factors may also affect lung function, a well known example of this being Cystic Fibrosis.

Irish Lung disease morbidity and mortality

Ireland has the highest death rate from respiratory disease in Western Europe (almost twice the EU average) with deaths now exceeding those from coronary artery disease. Respiratory disease kills one in five people in Ireland. The second most commonly reported long-term illnesses in young adults (under 44 years old) are conditions of the respiratory system. Lung cancer is the third most common cancer in both men and women. Survival rates for lung cancer are very low – the one year survival rate is 23.7% and the five year survival rate is 8.6%. Respiratory tuberculosis remains a significant problem although the incidence rate per 100,000 has remained largely unchanged since 2000 (20). Because of the increasing numbers

of deaths due to lung disease and the numbers of people living with chronic lung disease it has become increasingly important to study the mechanisms involved in both initial development and later function of the lung. By looking at what factors control lung function and development, we may gain clues as to what goes wrong in different conditions causing lung problems. Only by understanding what has gone wrong can we begin to devise solutions and potential new treatment options to prolong the life of affected individuals.

By looking at the signalling pathways which become activated following injury or tissue damage we may be able to come up with intervention strategies to limit any damage caused. We hypothesised that there may be a re-emergence of the pathways seen in the developmental stages in response to lung damage.

Lung Cancer

Lung cancer is the fourth most common cancer in Ireland. 20% of all cancer deaths in Ireland are from lung cancer and with the incidence among Irish women increasing, it is likely to become an even more prevalent disease (21). In theory, lung cancer is an almost preventable disease as 85-90% of cases have been attributed to smoking (21, 22)

The two main types of lung cancer are non-small cell lung cancer (NSCLC) (more common) and small cell lung cancer (SCLC) (15). SCLC is highly aggressive, almost always occurs in smokers and is rapidly growing. NSCLC is more variable and severity depends on its histological type (22). The prognosis for patients with lung cancer is primarily dependent on the stage of the tumour at the time of diagnosis. Patients diagnosed early with stage I tumours have a 40-70% survival following surgical resection (23).

Risk factors for developing lung cancer:

Smoking remains the leading risk factor and is associated with 90% of cases in women and 79% in men. Asbestos exposure is the most common occupational risk factor. Other factors include exposure to radon, arsenic, chromium, nickel. Pre-existing lung diseases such as tuberculosis, Chronic Obstructive Pulmonary Disease (COPD) and idiopathic pulmonary fibrosis also increase the risk of developing lung cancer (24).

Around 10% of lung cancers in asymptomatic patients are detected on chest radiographs, but most patients are symptomatic when diagnosed and can present with the nonspecific systemic symptoms of fatigue, anorexia, and weight loss (24). Table 1A below shows the treatment of lung cancer based on its stage.

Treatment of Lung Cancer According to Stage

<i>Stage</i>	<i>Primary treatment</i>	<i>Adjuvant therapy</i>	<i>Five-year survival rate (%)</i>
Non-small cell carcinoma			
I	Resection	Chemotherapy	60 to 70
II	Resection	Chemotherapy with or without radiotherapy	40 to 50
IIIA (resectable)	Resection with or without preoperative chemotherapy	Chemotherapy with or without radiotherapy	15 to 30
IIIA (unresectable) or IIIB (involvement of contralateral or supraclavicular lymph nodes)	Chemotherapy with concurrent or subsequent radiotherapy	None	10 to 20
IIIB (pleural effusion) or IV	Chemotherapy or resection of primary brain metastasis and primary T1 tumour	None	10 to 15 (two-year survival)
Small cell carcinoma			
Limited disease	Chemotherapy with concurrent radiotherapy	None	15 to 25
Extensive disease	Chemotherapy	None	< 5

Table 1A: treatment options for lung cancer by stage (24)

Evidence suggests that the Epidermal Growth Factor Receptor (EGFR) is involved in the development of various cancers. The EGFR and EGF-like peptides are often over-expressed in human carcinomas, and in vivo and in vitro studies have shown that these proteins are able to induce cell transformation. Evidence suggests that cooperation of multiple ErbB receptors and cognate ligands is necessary to induce cell transformation. In particular, the growth and the survival of carcinoma cells appear to be sustained by a network of receptors/ligands of the ErbB family. This phenomenon is also important for therapeutic approaches, since the response to anti-EGFR agents might depend on the total level of expression of ErbB receptors and ligands in tumor cells (25)

Our gene of interest, Mig-6, has been shown to be a negative regulator of EGF signalling so we were interested in looking at this pathway and what occurs when Mig-6 is ablated or knocked out.

1.2 Mouse Models to study disease development and progression

The use of mouse models allows us to manipulate various elements of the mouse genome to investigate factors involved in disease development and progression in addition to aspects of the oncogenic process. It also gives the chance to test potential therapeutic interventions. The success of a mouse model is dependent on its ability to target the specific oncogenic modification in a cell specific manner. The timing of the genetic modification is also crucial.

Mouse models are most commonly used to investigate the effect of specific gene ablation on the mouse. Two of those in use are conventional knockout models and conditional knockout models. Conventional models work on the basis of mutating or ablating endogenous genes by using homologous recombination in embryonic stem (ES) cells. Specific genes are targeted in vitro and the ES cells with the target modification are injected into 3.5 day old mouse

embryos. The ES cells incorporate themselves into the germline and the mutation is then transmitted to future generations of mice. The disadvantage of this method is that if the mutation introduced affects the ability of the mice to survive, the role of the gene in disease development or in the adult mouse cannot be studied.

Depending on the promoter used to express the transgene, initiation of expression of the transgene will be at different times. For example expression of genes under the control of the SP-C promoter is initiated at embryonic day 10 while genes under the control of a *CCSP* promoter are initiated at around day 17 of embryonic development. Expression of genes that disrupt the different developmental stages results in an embryonic lethal phenotype which makes those models of little value when one is interested in following the progression of a particular disease or cancer. (7, 8, 9)

Another limitation in using conventional mouse models is that once transcription of the transgene has been initiated it is irreversible. The ability to terminate transgene expression would allow identification of the stages of tumour progression independent of the growth promoting properties of the transgene.

As well as the lethal phenotype mentioned above, conventional models may also result in a number of non-lethal phenotypes:

- Artefacts can arise due to the lack of a gene product for the entire lifetime of the animal
- Presence of a selection marker can influence the phenotype of the mutation (26)

Conditional transgene models have overcome these limitations.

Conditional knockout models use tissue specific expression of recombinases to ablate genes in a cell and tissue specific manner. Site specific recombinases splice DNA segments which

are flanked by specific recognisable sequences. Homologous recombination in ES cells is used to insert recombinase recognition sequences around a gene of interest or regulatory exons. This technology is used to express site specific recombinases in a tissue specific manner. This allows the gene of interest, flanked by recombinase sites, to be deleted in a tissue specific manner (7, 8, 9, 10).

Site specific recombinases (SSRs) such as Cre and flp are capable of recombining specific sequences of DNA with high fidelity without the need for co-factors and have been used to create gene deletions, insertions inversions and exchanges. Both Cre and flp recombine DNA at defined target sites and are members of the λ integrase superfamily of SSRs (27).

Another commonly used recombinase is the PhiC31 phage integrase (a *Streptomyces* phage) (28)

For the purposes of our experiments we were interested in the Cre-loxP system.

Cre-loxP system:

The most common recombinase system in use is the Cre-LoxP system.

The Cre-lox mechanism was first observed in P1 bacteriophage where it is part of the normal viral life cycle allowing replication of its genomic DNA when reproducing. Since its discovery the Cre-lox system has been developed into a technology for genome manipulation (29). The site specific recombinase Cre of the bacteriophage PI recognises specifically 34bp long sequences called loxP (locus of X over in PI) (30). Cre excises a segment of DNA flanked by two loxP sites. Depending on the position and orientation of loxP sites several outcomes are possible- gene deletions, duplications, inversions and chromosome translocations. Mostly this system is used to conditionally activate or inactivate certain genes (31).

To be successful, Cre-lox requires only two elements to be present:

1. Cre Recombinases: catalyses recombination between two loxP sites
2. loxP sites: 34 base pair sequence containing two 13bp inverted repeats flanking an 8bp core sequence

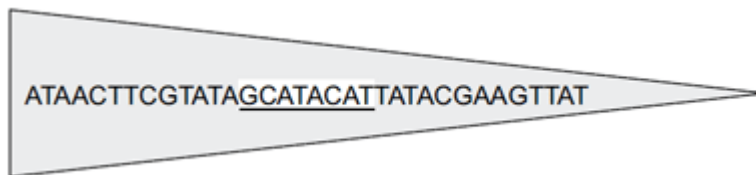


Figure 1.3: 34 base loxP sequence. The core sequence (shaded) is flanked by two inverted repeats (29)

This traditional type of Cre-lox system has a number of issues which can make it difficult to interpret the knockout phenotype (26):

1. If a selective marker is present it may have an influence on the phenotype of the mutation.
2. As the gene is knocked out for the lifetime of the transgenic animal, artefacts can develop.
3. Inactivation of some genes can cause lethality in utero which makes it impossible to look at the gene's function later in development or post-natally.

A variation of the Cre-lox system has found a way to potentially overcome these limitations. This version is a conditional gene targeting method based on the inducible activity of an engineered DNA recombinase. An inducible system allows control over the timing of the recombination event and also allows tissue specific removal of the target gene (26). In these inducible forms of Cre, the ligand binding domain of a mutated human oestrogen receptor

(ERT) (which recognises Tamoxifen and its derivatives but not normal oestrogen) is fused to Cre (31). This Cre-ERT is a functional Tamoxifen-dependent recombinase in cultured cells and in transgenic mice (26). By controlling the time point at which the target gene is excised using an inducible Cre recombinase, it allows us to look at the role of the gene later in the developmental process or in adult life as well as allowing tissue specific excision of the gene of interest. Studies have proven the validity of using the Tamoxifen dependent recombinase by showing excision of the gene in animals where the drug had been administered but no excision in animals that received no Tamoxifen treatment (26).

1.3 Cell Signalling

Overview of cell signalling:

Cell to cell communication in multicellular organisms is essential in order to ensure coordination of activities within the organism as a whole (32). Initiation of signal transduction occurs when a small molecule known as a ligand binds to its receptor protein often causing a conformational change in this receptor protein. Most signal receptors are plasma membrane proteins. There are many types of cell membrane receptors (32), three of which are listed below:

1. G-protein coupled receptors (GPCR)

GPCR contain 7 transmembrane alpha helical domains that bind to extracellular ligands via their extracellular domain. This in turn leads to a conformational change in their intracellular domain that results in the activation of G proteins in the cytoplasm by replacing GDP with GTP. This newly activated protein can then bind to another protein, which is usually an enzyme, and initiate the next step in the amplification of the signalling pathway. This activation is relatively short lived because the G protein contains endogenous GTPase activity that rapidly hydrolyses GTP to form GDP.

2. Receptor tyrosine kinases

These receptors have enzymatic activity within a cell and will be further discussed later.

3. Ion channel receptors

Ion-Channel Receptors are channel proteins in a plasma membrane that can open or close in response to a change in the local concentration of a ligand that binds specifically to the ion channel receptor. These channels are usually specific for a single ion (e.g. Ca^{2+} or Cl^-) are important in the functioning of the nervous system (33).

Receptor Tyrosine Kinases:

Receptor tyrosine kinases (RTKs) mediate cell-to-cell communication and are essential components of cellular signalling pathways which are active during both embryonic development and adult homeostasis. Many RTKs have been implicated in the onset or progression of various cancers, either through receptor gain of function mutations or through receptor/ligand overexpression (34).

RTKs are receptors which are found in the plasma membrane and are usually activated by ligand induced oligomerisation which juxtaposes the cytoplasmic tyrosine kinase domains. This allows autophosphorylation of tyrosine residues which in turn causes a conformational change which increases kinase activity (as shown in figure 1.4). Some phosphorylated tyrosine residues can attract various different downstream signalling proteins (enzymes and adapter proteins), typically through Src-homology-2 (SH2) or phosphotyrosine-binding (PTB) domains (34, 35).

Signal transduction pathways via receptor tyrosine kinases play pivotal roles in numerous aspects of physiological and pathological biology. The EGFR family, in particular, has been extensively studied as a prototype of RTKs since the 1980s (36).

Epidermal Growth Factor Receptor (EGFR):

EGFR and closely related family members, ErbB2, ErbB3 and ErbB4 are RTKs which send signals into the cell to regulate many critical processes (37). These receptors are at the apex of complex signal transduction cascades in a large number of cell types which modulate cell proliferation, survival, adhesion, migration and differentiation (38, 39).

Structure of EGFR

EGFRs are transmembrane receptors which have an N-terminal extracellular ligand-binding domain and a C-terminal cytoplasmic region which has enzymatic activity. This structure allows signals to be transmitted across the plasma membrane (39).

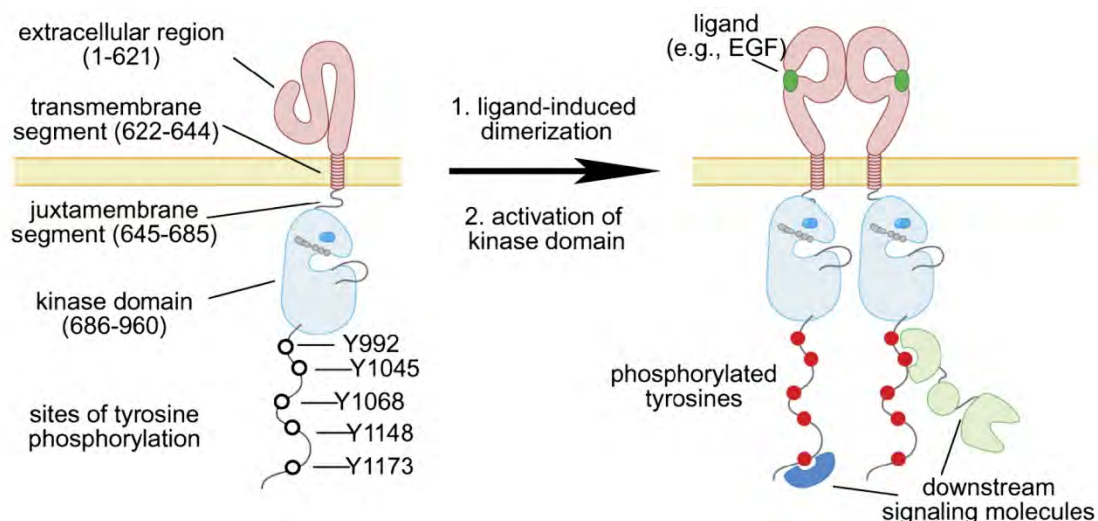


Figure 1.4: The above diagram shows a general view of the ligand-induced dimerization and activation process of EGFR (40)

Signalling via EGFR:

Signalling through the receptor begins when a ligand (EGF, EGF-like molecules, TGF- α and neuregulins) binds to the extracellular domain causing a conformational change and the signal is transmitted to the intracellular kinase domain. The kinase domain phosphorylates

several tyrosine residues in the C-terminal tail of the receptor which recruits PTB and SH2 domains containing signalling proteins and relays the signal to downstream signalling pathways (37)

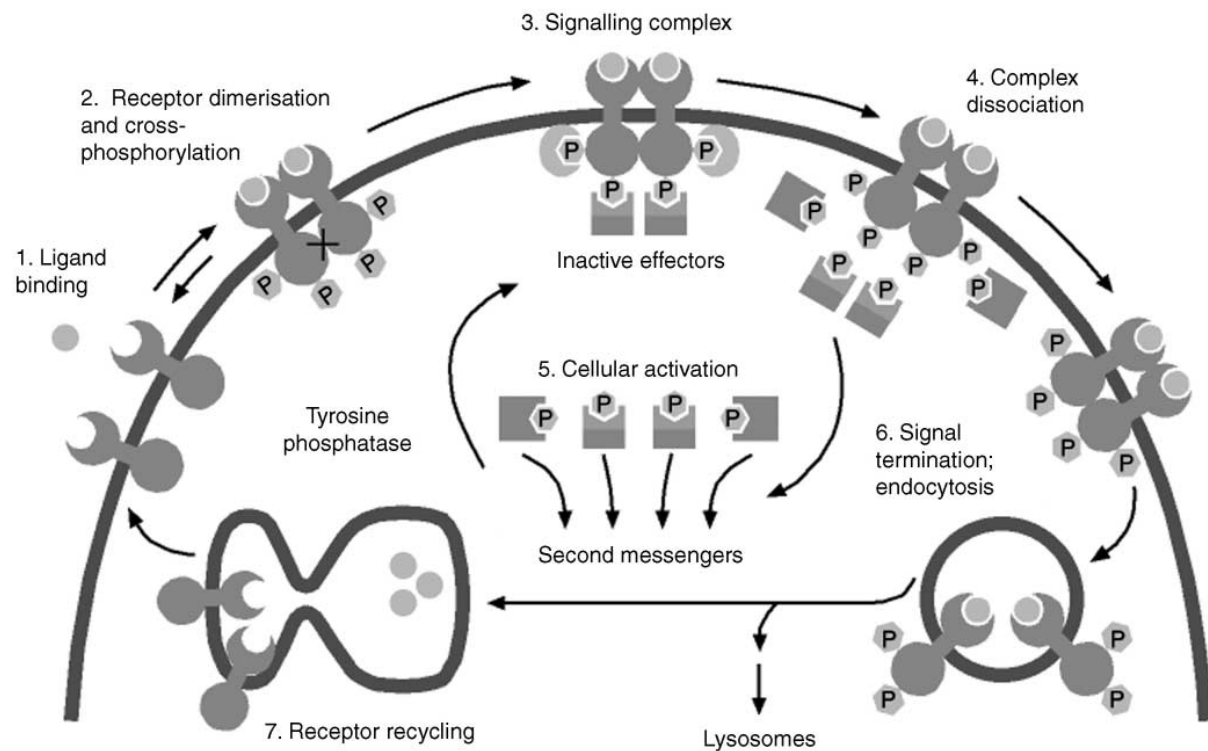


Figure 1.5: The epidermal growth factor receptor (EGFR) signal transduction model.

Ligand binding to receptors on the cell surface induces receptor dimerisation and cross phosphorylation. A transient signalling complex composed of effector and adaptor proteins is then assembled. Dissociation of this complex leads to an enzymatic cascade culminating in gene activation and a cellular response. During signal termination, ligand–receptor complexes are internalised through clatherin-coated regions of the plasma membrane and then either degraded or recycled to the cell surface (39).

EGF signalling is important in early and late stage lung development and its ablation leads to reduced lung branching and alterations in epithelial cell population (41). EGF can also activate downstream signalling, Ras-PI3K/Akt and Ras/MAPK and cross-talk with other

growth factors such as TGF- β 1 and HGF signalling which are all important in lung development (5).

Feedback inhibition of EGFR signalling:

Signalling networks need to be coordinated in a strictly controlled manner and negative regulators have been shown to have an important role in this regulation. Continuing research has shown that a number of negative regulators exist which play major roles in regulating signalling networks via multiple modes of action. The coordinated action of positive and negative regulators provides the fine tuning necessary to maintain correct signalling pathways (42). It has been seen that loss or decrease in expression of negative regulators can be linked to cancer development (36).

Negative regulators of EGFR signalling include the following:

- Mitogen inducible gene 6 (Mig-6)/RALT/Gene 33 (43)
 - o This is an early-response gene induced by EGF. Its transcription is induced by the extracellular signal-regulated kinase (ERK) pathway that is activated by growth factors such as EGF or by multiple stimuli, including osmotic and mechanical stress. Mig-6/RALT/Gene 33 binds to the tyrosine kinase (TK) domains of EGFR and ErbB2 and inhibits TK activity.
 - o Studies of the crystal structures that form between Mig-6 and the kinase domain of EGFR have shown that an approximately 25 residue epitope of Mig-6, known as segment one, binds to the distal surface of the C lobe of the kinase domain. Other analyses (biochemical and cell based studies) confirm that this interaction, seen on examination of the crystal structures, contributes

to EGFR inhibition by blocking the formation of the activating dimer interface. (44, 45)

- Fibroblast growth factor receptor substrate 2 beta (FRS2 β)
 - o FRS2 β constitutively binds to EGFR, regardless of ligand stimulation. After activation of ERK by various growth factors, including EGF, the phosphorylated ERK binds to FRS2 β and inhibits EGFR autophosphorylation and signal transduction. Thus, FRS2 β acts as a negative feedback regulator of EGFR (46).
- Suppressor of cytokine signalling 3 (SOCS3)/SOCS4/SOCS5
 - o Is an early-response gene induced by EGF. SOCS proteins are negative feedback regulators of EGFR. They bind to autophosphorylated EGFR via their SH2 domains and recruit E3 ubiquitin ligase complex via their SOCS domains, leading to the ubiquitinylation and degradation of EGFR(47).
- Leucine-rich repeats and immunoglobulin-like domains 1(LRIG1)
 - o An early-response gene induced by EGF. LRIG1 acts as a negative feedback regulator of EGFR (48). It binds to EGFR via its extracellular domain and recruits Cbl – an E3 ubiquitin ligase – via its cytoplasmic domain, leading to the ubiquitinylation and degradation of EGFR (36).

The modes of action of these inhibitors are shown in figure 1.6 below

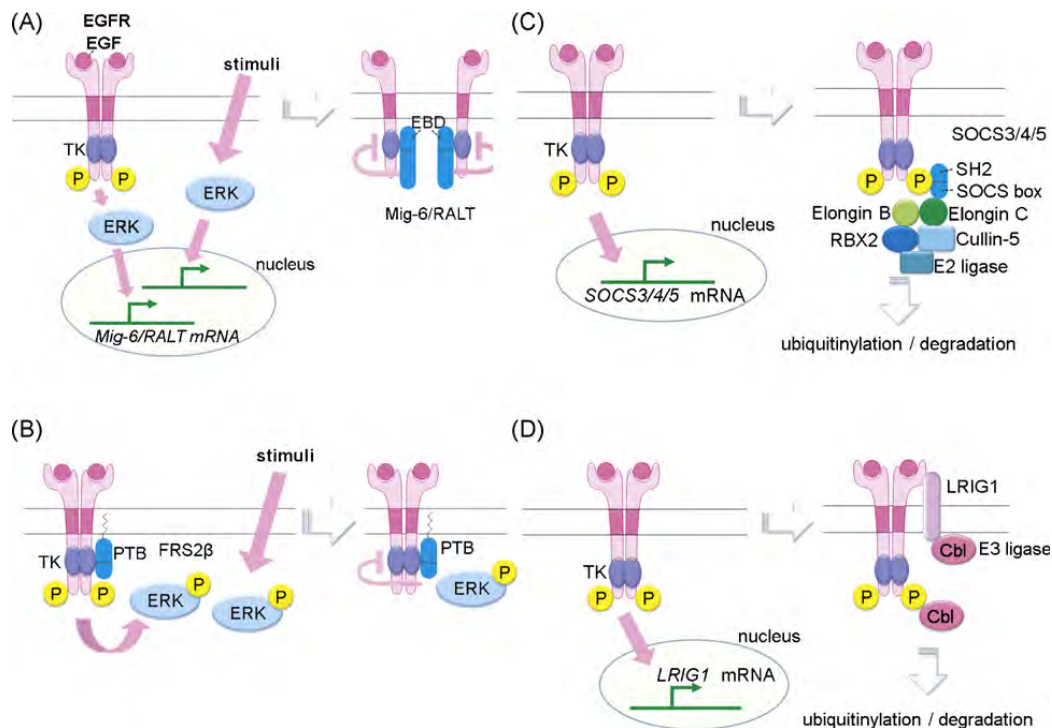


Figure 1.6: Multiple modes of action of the inhibitors. (A) *Mig-6/RALT* transcription is induced by the activation of ERK pathway via activated EGFR or other stimuli. The translated Mig-6/RALT binds to the activated TK domain of EGFR and ErbB2 and inhibits the TK activity. (B) FRS2 β constitutively binds to EGFR. Activated EGFR or other stimuli activate the ERK pathway. The activated ERK binds to FRS2 β and inhibits the EGFR signalling. (C) *SOCS3*, *SOCS4*, or *SOCS5* transcription is induced by stimulation with EGF. The translated SOCS3/SOCS4/SOCS5 binds to the autophosphorylated EGFR via its SH2 domain and recruits the E3 ubiquitin ligase complex via its SOCS box. (D) *LRIG1* transcription is induced by stimulation with EGF. The translated LRIG1 binds to EGFR family members via its extracellular domain and recruits Cbl E3 ubiquitin ligase to its cytoplasmic tail, inducing ubiquitinylation/degradation of the EGFR family members (36)

HGF signalling:

Hepatocyte growth factor/scatter factor (HGF) is a multifunctional factor produced by many cell types, including normal fibroblasts, epithelial and endothelial cells, but also different oncogenic cells.

Mesenchymal-epithelial tissue interactions are important for development of various organs, and in many cases, soluble signalling molecules may be involved in this interaction. Hepatocyte growth factor (HGF) is a mesenchyme-derived factor which has mitogenic, motogenic and morphogenic activities on various types of epithelial cells and is considered to be a possible mediator of epithelial-mesenchymal interaction during organogenesis and organ regeneration. It has been suggested that HGF is a putative candidate for a mesenchyme-derived morphogen regulating lung organogenesis (49).

HGF has been reported to influence cell proliferation of hepatocytes and multiple other cell types, kidney cell migration, organ and tissue development, but also the invasiveness of tumour cells and other biological responses (50, 51). HGF binds to the receptor tyrosine kinase c-Met which transmits the HGF signal into the cytoplasm (52). c-Met autophosphorylation leads to the recruitment of signal transduction proteins like the c-Src kinase, phospholipase C-g, the Grb2zSoS complex, and phosphatidylinositol 3-kinase (51).

The mature HGF protein binds to its high-affinity receptor c-MET, leading to its activation and phosphorylation of multiple serine and tyrosine residue sites. The extracellular Sema domain of c-MET mediates binding to the ligand HGF, which, subsequently, leads to receptor dimerisation and activation of its intrinsic tyrosine kinase. The c-MET/HGF pathway has gained considerable interest through its apparent deregulation by overexpression or gain-of-function mutations in c-MET in various cancers, including lung cancer (53, 54). The figure below (1.7) illustrates the interaction of HGF and c-MET and the resulting pathways which are stimulated (54).

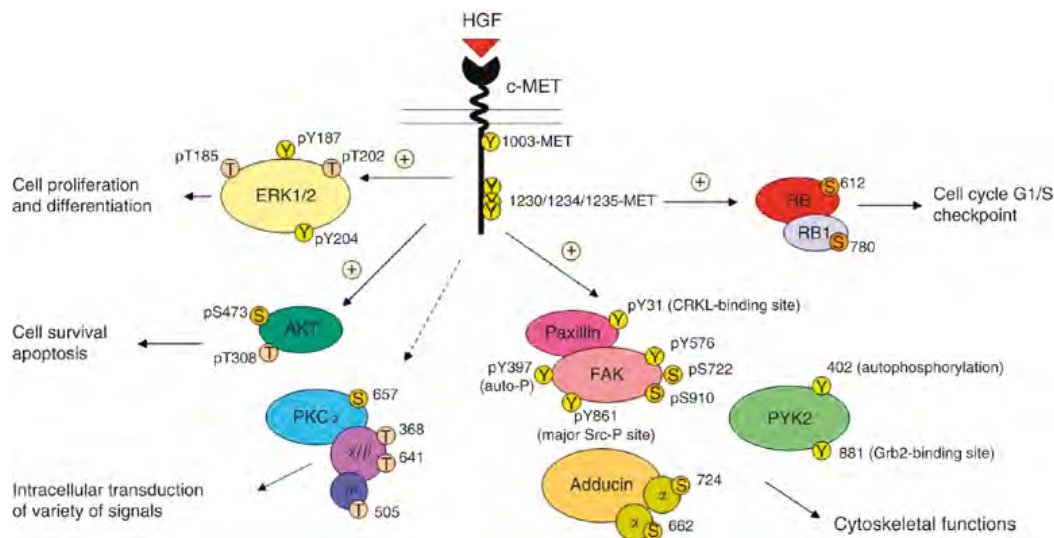


Figure 1.7: shows the versatile signalling functions of c-MET/HGF pathway regulating various biological functions of the cells, including cytoskeletal functions, cell proliferation and differentiation, survival, and apoptosis. Various potential serine, threonine and tyrosine phosphorylation sites on the signalling phosphoprotein intermediates are included (54).

The ability of HGF to stimulate mitogenesis, cell motility and matrix invasion means it has a central role in angiogenesis, tumourogenesis and tissue regeneration (51). There is evidence that HGF plays an essential part in parenchymal repair and protection in various organs. In the lungs, HGF is a potent regenerative and cytoprotective factor during organogenesis or in cases of acute injuries (55). c-MET is normally expressed by epithelial cells but is also found on endothelial cells, neurons, hepatocytes, haematopoietic cells and melanocytes. HGF expression is restricted to cells of mesenchymal origin (49, 56).

1.4 Mig-6

Mig-6 is an immediate early response gene (& adapter protein) that is transcriptionally induced by a divergent array of extracellular stimuli including various growth factors, cytokines and stress factors as well as by the Ras oncoprotein (1, 2, 3). Mig-6 is also known as receptor associated late transducer (RALT), gene 33 (in rat) and ERBB feedback inhibitor 1 (ERFFI1) (2). Mig-6 has been mapped to human chromosome 1p36 and to the distal region of mouse chromosome 4 (4). The Mig-6 gene spans ~13.8kb and contains four exons including the non-coding exon 1 and the coding exons 2-4. The Mig-6 full length transcript is 3.1kb and encodes a protein of 461 amino acids (6).

At least five functional regions have been identified in the Mig-6 gene which are:

1. Threonine/serine phosphorylation region
2. Src-homology 3 (SH3) binding domain
3. Cdc42/Rac interaction and binding (CRIB) domain
4. 14-3-3 binding domain
5. ErbB-2 binding domain (5)

The Mig-6 gene has a number of features including the following: it is present only in higher animals such as humans and rodents but not in lower ones like *Drosophila* or *C.elegans*. This suggests that Mig-6 was acquired during evolution for regulating more complex signalling networks. Secondly, since it is an immediate early response gene its expression can be rapidly induced, it may play an important role in early regulation of cellular responses (4).

Transcriptional regulation of Mig-6:

Mig-6 expression can be induced by a wide variety of external stimuli, a summary of some of which are listed in table 1B below

<u>Transcriptional inducers of Mig-6 expression</u>		
Growth Factors	Stresses	Hormones/Others
EGF	Diabetic nephropathy	Glucocorticoids
FGF	Hypoxia	Insulin
HGF	Live <i>Staphylococcus</i> infection	Retinoic acid
TGF- α	Ventilator induced lung injury	Alklyating agents
PDGF	Mechanical strain	cAMP

Table 1B: Summary of the transcriptional inducers of Mig-6 expression (4)

Various inducers can differentially activate the regulation of Mig-6 and may use different intracellular pathways to accomplish this regulation. The induction of Mig-6 by growth factors such as EGF is mediated via the Ras-MEK-ERK pathway. The MEK-ERK pathway is also responsible for Mig-6 induction by serum, phorbol and sorbitol induced osmotic stress. Regulation of insulin induced Mig-6 expression varies in different cell types. The PI-3K and ERK pathways are involved in hypoxia induced Mig-6 expression (4).

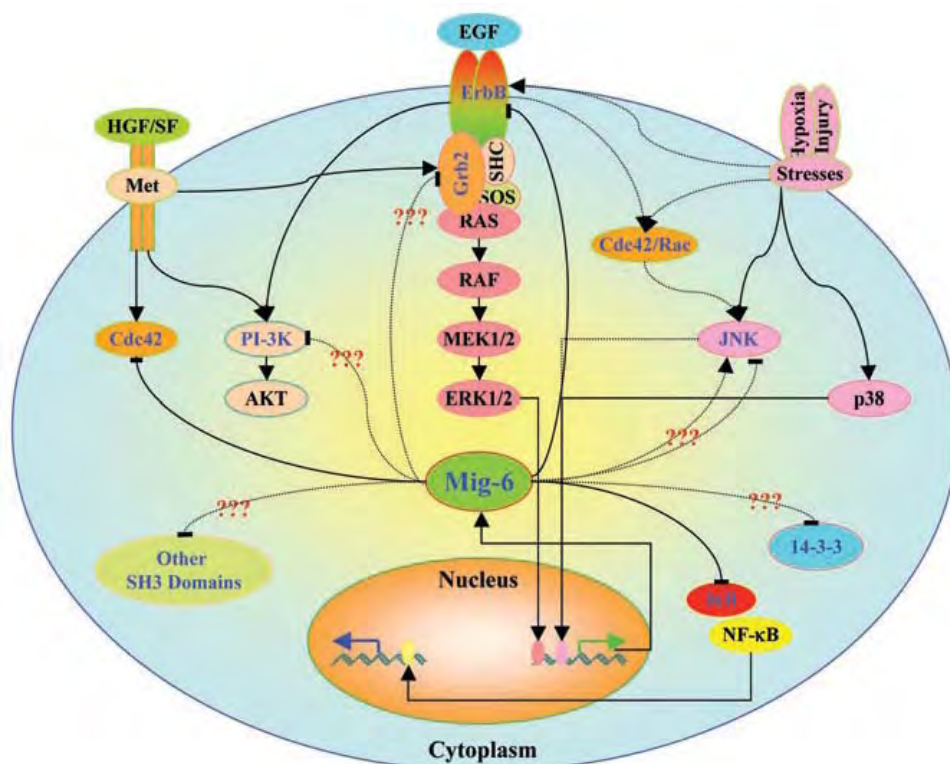


Figure 1.8 shows the known and potential actions of Mig-6 on the EGF, HGF/SF and certain stress induced signal transduction.

Mig-6 in development, homeostasis and stress response:

Mig-6 expression levels differ among different tissues and also in the same tissues at different time points during foetal development and adult maturation. The mouse liver contains high levels of Mig-6 while varied levels are present in the lung, placenta, heart, brain, stomach and skeletal muscle. The foetal liver shows low levels of Mig-6 expression while a sharp increase is observed in the newborn liver (this suggests that, at birth, the hepatocytes respond to hormonal and/or environmental changes) (4). The level of Mig-6 expression in the lung differs throughout the gestational period as can be seen in Figure 1.9 below:

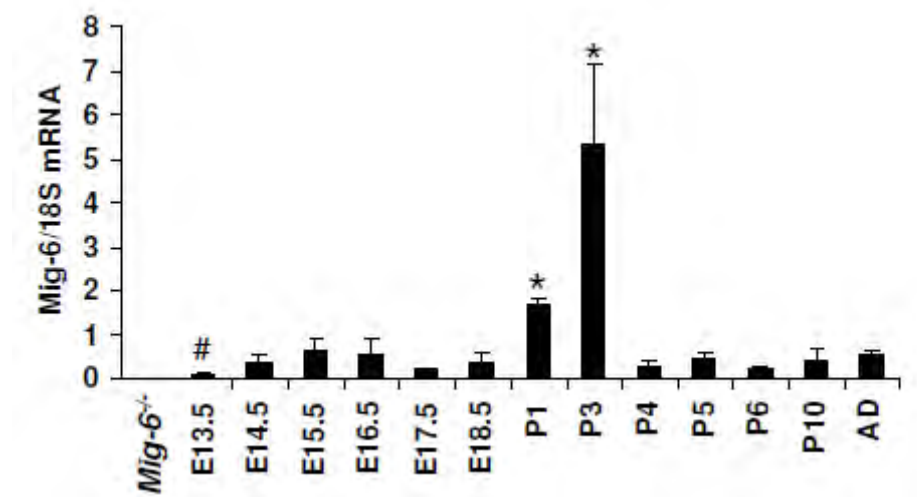


Figure 1.9: Differential expression of *Mig-6* during murine lung development. (A) *Mig-6* relative mRNA levels in E13.5, E14.5, E15.5, E16.5, E17.5, E18.5, P1, P3, P4, P5, P10, and adult (3-month-old, AD) lungs by quantitative real-time RT-PCR. (5)

E13.5→E18.5: embryonic day 13.5-day 18.5. P1→P10: pups day 1→10.

In mice, genomic disruption of the *mig-6* gene leads to degenerative joint diseases, skin cancer, lung cancer and gastrointestinal tract tumours. It has been demonstrated that ablation of *Mig-6* results in a partial lethal phenotype with 50% of these mice dying during the neonatal period (5).

Mig-6 is a negative regulator of EGF signalling

Mig-6 can be transcriptionally induced by EGF, and it acts as a negative feedback inhibitor of EGF receptor signalling by blocking formation of the activating dimer interface (44). *Mig-6* interacts with the EGFR *in vivo* in an EGF-inducible manner (58). Overexpression of *Mig-6* *in vitro* leads to inhibition of ErbB2 autophosphorylation and reduced MAPK pathway activity, through binding of *Mig-6* to ErbB receptors (2).

The C-terminal region of *Mig-6* contains a segment (residues 323-372) which is essential for EGFR and ErbB2 binding. Studies of the crystal structure of the area around this segment has

defined a 25-residue epitope of Mig-6 that binds to the EGFR (ErbB2) kinase domain and has been given the term segment 1. The footprint of Mig-6 (segment 1) on the kinase domain of EGFR overlaps the cyclin-like face of the kinase domain in the asymmetric kinase domain dimer, and so binding of Mig-6 to an EGFR kinase domain will prevent it from acting as a cyclin-like activator for other kinase domains. Residues in the Mig-6 binding interface of EGFR are conserved suggesting that Mig-6 could potentially bind to other members of the EGFR family. Introduction of individual mutations in Mig-6 (segment 1) interrupts the binding of EGFR and Mig-6, proving that it is segment 1 which is important for inhibition of EGFR. An interesting property of Mig-6 is its ability to bind more tightly to activated EGFR than to the unbound receptor (44).

Mig-6 as a tumour suppressor gene

Mig-6 localises in human chromosome 1p36, a locus that has been widely suggested to harbour putative tumour suppressor genes including EXTL1 (a candidate neuroblastoma suppressor gene) as well as p73, the p53 tumour suppressor gene homolog. No mutations in p73 have been identified in human lung cancer so it can be discarded the responsible tumour suppressor in the lung. Allelic imbalance of chromosome 1p36 is one of the most frequent genetic alterations observed in various human cancers (3).

It is plausible to consider Mig-6 as a potential tumour suppressor gene for many different reasons, some of which are listed below:

- It is located on chromosome 1p36.12-36.33, a locus considered a hot spot of allelic imbalance for lung cancer (3)
- Loss of function mutations in Mig-6 have been identified in human lung cancer cell lines

- It is negative regulator of receptor tyrosine kinase signalling from EGF and HGF, whose receptors have been shown to play important roles in lung malignancy (3)

Mig-6 knock-out models have been developed in order to further study the role of Mig-6 in different organs both during foetal development and after birth into adulthood. One such model has been generated in the DeMayo laboratory at Baylor College of Medicine. The embryo lethal phenotype and multi-tissue carcinogenesis of the Mig-6 null allele make it difficult to investigate the impact of ablation of Mig-6 on specific tissue and at specific time points in development. In order to look at the role of Mig-6 in specific tissues, a conditional knock out model would be useful. The DeMayo lab have successfully generated a conditional null allele, Mig-6^{f/f}, by introducing LoxP sites that flank exons 2 and 4 of the Mig-6 gene. The Mig-6 conditional null allele was validated in the recombined Mig-6^{-/-} mice by measuring Mig-6 mRNA and protein in the liver, lung, uterus and skin. Neither mRNA nor protein of Mig-6 could be detected by real time RT-PCR or Western blot analysis in the liver, lung, uterus and skin of recombined Mig-6^{-/-} mice (34). The recombined Mig-6^{-/-} mice developed pathological changes such as degenerative joint diseases and skin hyperplasia, similar to the previously reported Mig-6 germline null allele. These mice also had enlarged uteri with endometrial hyperplasia. This Mig-6^{f/f} mouse is used as a valuable tool in the study of Mig-6 in a tissue specific manner (6).

Aims:

We approached our work with two main aims which were to use animal studies and cell studies to look at the role of Mig-6.

In our animal studies we planned to use the previously mentioned conditional knockout model to look at what occurs in murine lungs when Mig-6 is ablated. We would analyse our results using quantitative real time pcr and Western blot analysis.

The cell studies would focus on epithelial and endothelial cells. We aimed to knockdown Mig-6 expression in these cells using siRNA to determine what effects (if any) this would have on cellular survival and also what pathways may be involved in response. We would also look at EGF stimulation studies in both cell types. Again we would look at our results using real time pcr and Western blot analysis.

2. Materials and Methods

Animal strains used:

We used the Mig-6^{f/f} mice in order to study the role of Mig-6 in adult mice by developing an inducible ablation model which produced our Mig-6^{d/d} mice. To obtain our Mig-6^{d/d} mice, *Rosa26-Cre-ERT2* mice were crossed with *Mig-6flox/flox* mice and the resulting *Rosa26-Cre-ERT2; Mig-6flox/flox* (Mig-6^{d/d}) or *Mig-6flox/flox* (Mig-6^{f/f}) mice (2 months old) were injected peritoneally with 1 mg of Tamoxifen for 5 days. These mice were further maintained for 4 months before analysis. It was expected that in the Mig-6^{d/d} mice Mig-6 would have been successfully ablated. At six months old mice were sacrificed, lung tissue harvested and our experiments carried out.

2.1: siRNA treatment of epithelial and endothelial cells

Materials

- siRNA (Thermo Scientific, Dharmacon)- ON-TARGET plus SMART pool human Mig-6
- Penicillin/Streptomycin (100X) (GIBCO)
- Lipofectamine 2000 reagent (Invitrogen)
- Opti-MEM (Invitrogen)
- Culture Plates (Grenier labortechnik)
- RPMI 1640 (Invitrogen)
- FBS (Invitrogen)

2.1 siRNA treatment of epithelial and endothelial cells

siRNA treatment was carried out on these epithelial and endothelial cells in order to knock down Mig-6 and investigate the effect (if any) this would have on genes downstream from Mig-6 in signalling pathways. We were also interested to see whether knocking down Mig-6 would affect cell viability. Protein and RNA were isolated from the treated cells for Western blot and real time PCR analysis.

The H441 human bronchiolar epithelial cells (National Cancer Institute, Frederick, MD) were grown in RPMI 1640 (+ 10% FBS + P/S (penicillin/streptomycin)) until 40% confluency. Human lung micro vascular endothelial cells (HMVEC-L, Lonza, Walkersville, MD) were maintained in Endothelial Cell Medium containing hEGF, hydrocortisone, GA-1000, FBS, VEGF, hFGF-B, R3-IGF-1, and ascorbic acid (Bullet Kit, Lonza) until 60% confluency.

Cells were cultured in the Tissue Culture Core (TCC) at Baylor College of Medicine. Culture medium was RPMI 1640 medium supplemented with 2 mM L-glutamine, 1.5 g/l sodium bicarbonate, 4.5 g/l glucose, 10mM HEPES (pH 7.4), 10% foetal bovine serum, and 1%v/v antibiotics to prevent bacterial growth. Cells were cultured at 37°C in 5% CO₂ and passaged every 3 days.

Cells were transfected with 50 nM of control siRNA or SMART pool of human Mig-6 siRNA (Dharmacon, Chicago, IL) in serum-free OptiMEM (Invitrogen, Carlsbad, CA).

For each 6 well culture plate the following steps are carried out.

33µl of lipofectamine with 660µl of opti-MEM is mixed (by pipetting ~50 times) and left to settle for 30mins. To each of six microtubes 100µl of opti-MEM was added along with the volume of siRNA required to give a final concentration of 50nM. 100µl of opti-MEM containing lipofectamine was added to the opti-MEM containing siRNA mixed by pipetting

approx. 50 times and left to settle again for 30 min. A tube containing opti-MEM, 2% FBS, and 1% v/v antibiotics was prepared. 800 µl of opti-MEM containing 1x antibiotics plus 2% FBS was added to the lipofectamine siRNA mixture. 1000 µl of opti-MEM with 2% FBS, lipofectamine and siRNA mixture was added to each well. After overnight culture, 1 ml of RPMI 1640 medium containing 20% FBS and 1% antibiotics was added to each well and culture continued for a further 48hrs. Following culture, protein and RNA were isolated from the cells for Western blot and real time PCR analysis.

2.2 EGF/HGF induction of Mig-6 in siRNA treated cells

Materials

- 40ng/ml EGF
- 40ng/ml HGF
- BEBM (bronchial epithelial cell basal medium) (Lonza)
- Protein Lysis Buffer (10 mM Tris HCl, pH 7.5, 5 mM EDTA, 50 mM NaCl, 0.1% NP40, 1 mM PMSF, 10 µg/ml aprotinin, and 10 µg/ml leupeptin)- Sterile PBS pH7.4- Cell Star macroplate with lid (Grenier labortechnik)
- opti-MEM (GIBCO)

2.2 EGF/HGF induction of Mig-6 in siRNA treated cells

NHBE (normal human bronchial epithelial) cells were cultured (in BEBM) and subjected to siRNA treatment to knock down Mig-6 as detailed for the H441 and HMVEC cells in section 2.1. The siRNA treated cells in culture at ~50% confluency were then subjected to treatment with 40ng/ml of EGF (epidermal growth factor) and HGF (hepatocyte growth factor) (24hrs post siRNA treatment) to investigate what effect, if any, addition of these substances would

have on Mig-6 and other protein levels. siRNA silences Mig-6 expression but it was hypothesised that addition of either EGF or HGF could induce expression of Mig-6 once again and levels would increase post administration of the growth factors.

Stock solutions of EGF (100µg/ml) and HGF (10µg/ml) were firstly diluted to a concentration of 40ng/ml in opti-MEM medium. After siRNA treatment was complete (72hrs), the media was removed from each culture well, rinsed with opti-MEM and 1ml of either EGF 40ng/ml or HGF 40 ng/ml was added. Culture plates were incubated at 37°C with 5% CO₂ for 0mins, 15mins, 30mins, 1 hr, 2hrs and 4hrs. At each of the above time points the treated cells were harvested for protein.

2.3 SDS PAGE and Western blot

Materials:

- Protein marker- Precision Plus Protein Standards (BIO-RAD)
- Gel:
 - o BIO-RAD ready gel, precast gel for electrophoresis (BIO-RAD)
- Mini-Trans Blot Electrophoretic Transfer Cell (BIO-RAD) Gel transfer cell, gel holder cassettes, fibre pads, electrodes, tank, cooling unit, lid with cables
- Milk- Nestle Carnation instant non fat dry milk powder
- Weighing scales TR 603D, (Denver Instrument Company)
- X-Ray film- HyBlot Cl Premium autoradiography film (Denville Scientific Inc.)
- Autoradiography Cassette (Fisher Scientific)
- RestoreTM Western blot Stripping Buffer (Thermo Scientific)
- AmershamTM ECL Plus Western blotting detection system (GE Healthcare)
- PVDF Membrane (0.45µm), Immobilon-P transfer membrane (Millipore)

- Gel Filter Paper (Whatman)
- PBS:
 - o 1LH₂O
 - o 8g NaCl (Sigma)
 - o 80ml Phosphate buffer pH 7.4 (Sigma)
- PBST (Wash Buffer)
 - o 1L PBS
 - o 20μl 20% Tween 20 (Fisher Scientific)
- Blocking Buffer:
 - o 100ml PBST
 - o 1g non-fat dry milk (Nestle)
- 10x TBS
 - o 200ml 1M Tris-HCl (pH 7.5)
 - o 300ml 5M NaCl
 - o 500ml H₂O
- Alternative wash buffer (TBST)
 - o 1x TBS with 0.1% Tween-20
- Alternative blocking buffer
 - o 100ml 1x TBST
 - o 5g non-fat dry milk (Nestle)
- 5X running buffer:
 - o 15.1g Tris

- 94g glycine
- 50ml 10% SDS
- Make up to 1000ml with water
- 1x transfer buffer:
 - 2.9g glycine
 - 2.8g Tris
 - 200ml methanol
 - Adjust to 1000ml with water

Primary antibodies:

- Anti- Met, rabbit polyclonal (Santa Cruz Biotechnology)
- Anti-EGFR, rabbit polyclonal (Santa Cruz Biotechnology)
- Anti- Akt, Mouse monoclonal (Santa Cruz Biotechnology)
- Anti- p-Akt (Ser 473), rabbit polyclonal (Santa Cruz Biotechnology)
- Anti-RALT/MIG-6 (PE-16), rabbit polyclonal (Sigma Aldrich)
- Anti- Actin, mouse monoclonal (clone AC-40) (Sigma Aldrich)

Secondary antibodies:

- Peroxidase labelled rabbit anti-mouse IgG (Santa Cruz Biotechnology)
- Peroxidase labelled goat anti-rabbit IgG (Santa Cruz Biotechnology)
- Protein lysis buffer
 - (10 mM Tris HCl, pH 7.5, 5 mM EDTA, 50 mM NaCl, 0.1% NP40, 1 mM PMSF, 10 µg/ml aprotinin, and 10 µg/ml leupeptin)
- Eppendorf tubes
- Heating block (Fisher Scientific)

- Parafilm

2.3 SDS PAGE and Western blot

Protein Isolation from siRNA treated cells:

To harvest the proteins the following was carried out: media was removed from the appropriate well and 100µl of protein lysis buffer added. A pipette tip was used to scrape the bottom of the culture well to remove all cells and ensure complete homogenisation. The cell lysates were transferred to labelled eppendorf tubes, covered with parafilm and boiled for 5 mins to inactivate endogenous enzyme activity such as phosphatase activity.

In the case of our time course studies 100µl of PBS (pH7.4) was added to the resulting empty culture well and the remaining cells in the culture plate placed back in the 37°C incubator until the next time point for protein harvesting. In all cases the amount of protein harvested was measured to allow us to adjust our loading to ensure equal protein amounts were loaded onto the gel. The lysates could be immediately used for Western blot analysis or frozen at -20°C for future analysis.

Western blot was used to analyse the protein samples collected from H441 epithelial cells, HMVEC cells and NHBE cells. We wanted to look at the effect knocking down Mig-6 had on Akt, p-Akt, mTor, p-mTor, c-Met, EGFR and p-EGFR levels in our cells..

The running apparatus was prepared and the gel inserted into the cassette and the comb removed. The cassette was placed into the tank and 1x running buffer poured in until all wells were fully submerged. 5µl of protein marker was added to well number one. 20µl of sample was added to the remaining wells. The apparatus was connected to a power supply and run at a constant voltage of 100V for approximately two hours. Once the dye front had run approx. 2/3 of the length of the gel the protein was transferred to a PVDF membrane as follows: one edge of the membrane was labelled and the entire membrane was then submerged in

methanol. The transfer apparatus was assembled (Black side of cassette down, sponge, filter paper, gel, membrane, filter paper, sponge), ensuring there were no air bubbles between layers to hinder an efficient transfer. Once assembled, the transfer apparatus was placed into the tank. An ice pack was placed in the tank and transfer buffer poured in until the cassette containing the gel and PVDF membrane was completely covered. This was run at 50-60V for two hours.

Blocking Step:

Following the transfer step, the membrane was rinsed briefly with PBS. This was followed by blocking in blocking/staining solution for one hour at room temperature on a plate rocker.

Primary antibody:

Antibodies were diluted as required- 1:1000 in blocking/staining solution. Following the blocking step, the diluted primary antibodies were applied to the membrane (10ml per membrane). Primary antibody was incubated at 4°C overnight on a plate rocker.

Washing step:

The following day the membrane was washed with PBST for ten minutes at room temperature on a plate rocker. This wash solution was discarded and the wash step was repeated twice to ensure sufficient washing was achieved.

Secondary Antibody

Following the wash step, enzyme-conjugated secondary antibody raised against the primary antibody was applied (at a dilution of 1:1000). Secondary antibody incubation was for one hour at room temperature on the plate rocker. Following secondary antibody incubation, the membrane was washed again as detailed above.

ECL treatment:

In order to be able to visualise the protein bands, lumigen must be applied to the membrane. For each membrane ~1ml of lumigen is required. 1ml of lumigen A (GE Healthcare ECL Plus Western blotting detection system) was mixed with 25 μ l of lumigen B. The lumigen mixture was applied to the membrane and incubated for two to three minutes. The membrane was then transferred to an autoradiography cassette.

In the dark room an autoradiograph film was placed on top of the membranes. Initial exposure time was ten mins and then reduced or increased depending on the result seen upon development of the first film. Films were developed by placing the exposed film into the processor and protein banding patterns were observed. Digital copies of the negatives were taken using a Sony 10 mega pixel camera and a white light box to back-illuminate the film.

Stripping the membrane for re-use:

In order to re-use the membrane and apply a new set of antibodies all primary and secondary antibodies bound to antigen on the membrane needed to be first stripped from the membrane. To do this we used a commercial stripping buffer (containing beta-mercaptoethanol) which strips off the primary and secondary antibodies while leaving the protein sample on the PVDF membrane. Approximately 5ml of stripping buffer was applied to the membrane and incubated for 15mins on the plate rocker at room temperature. Following stripping, the membrane was rinsed with PBS and blocked with 1% milk for 1 hour at room temperature followed by the new primary antibody for one hour at room temperature. From this point on the procedure was followed exactly as detailed above.

Western blot- alternative procedure:

We began having difficulties with some of our Western blot results so we decided to optimize the method to enable us to get better, more reproducible results. These changes will be detailed here and referred to in the relevant results section:

Changes were made to the buffers and blocking solution used. Instead of using PBST we switched to TBST (Tris buffered saline & 0.1% Tween) for our washing steps and also for making our blocking solution. Instead of blocking with 1% milk in PBST for one hour we instead just briefly rinsed the membrane with 5% milk in TBST. Antibodies were diluted in 5% dry milk powder (w/v) in TBST instead of 1% dry milk powder (w/v) in PBST. For each wash step we reduced the length of time from ten minutes to eight.

2.4 RNA Isolation

Materials:

- TRIzol® reagent (Invitrogen)
- Chloroform (Fisher Scientific)
- Isopropanol (Fisher Scientific)
- 70% ethanol (PHARMACO-AAPER)
- Microcentrifuge tubes
- Pipettes -P1000, P200, P20 (Gilson)
- Centrifuge
- UV spectrometer
- TipOne pipette tips (USA scientific Inc.)
- DEPC treated water

2.4 RNA Isolation

RNA was isolated from siRNA treated cells and also from frozen mouse lung tissues. The RNA was used for real time PCR analysis.

Prior to RNA Isolation from samples, the bench area, pipettes, other instruments and gloves were sprayed with 70% ethanol to avoid RNase contamination and maximise the amount of RNA isolated from the samples. All dilutions were made using DEPC treated water.

Cultured cells were lysed directly in the culture dish by adding 1ml of TRIzol® reagent to a 3.5cm diameter dish, and the cell lysate was passed through a pipette several times. The homogenised samples were incubated at room temperature for five minutes to allow complete dissociation of nucleoprotein complexes. 0.2ml of chloroform (**Fisher Scientific**) was added, sample tubes capped securely and tubes shaken vigorously (by hand) for ~15 seconds. Samples were incubated at room temperature for two to three minutes and then centrifuged at 12,000 x g for 15 minutes at 4°C. Following centrifugation the sample separated into a lower red phenol–chloroform phase, an interphase and a colourless upper aqueous phase (containing the RNA). The aqueous phase was transferred to a fresh tube and RNA precipitated by addition of 0.5ml isopropyl alcohol (**Fisher Scientific**). Samples were incubated at room temperature for ten minutes to precipitate RNA and then centrifuged at 12,000x g for ten minutes at 4°C. After centrifugation the RNA forms a gel-like pellet on the side and bottom of the tube. The supernatant was removed and the RNA pellet washed with 1ml 70% Ethanol (**PHARMCO-AAPER**). Sample was mixed by vortexing (**Fisher Scientific**) and then centrifuged at 7,500 x g for five minutes at 4°C. After ethanol wash, the pellet was briefly dried by vacuum. RNA was dissolved in 30µl DEPC (Diethylpyrocarbonate) water. RNA was then quantified by UV spectrometry. An aliquot of each sample was diluted 1 in 65 with a final volume of 260µl (4µl RNA in 260µl water)

RNA was isolated from frozen lung tissue in essentially the same manner as for cells, with the following exception. When isolating RNA from the tissue samples, after addition of TRIzol® reagent (per lung) the tissues were homogenised and placed on ice until all samples had been homogenised. From this point, the procedure was the same as for the cultured cells.

2.5 Quantitative Real Time PCR

Materials:

- 5x first strand buffer (Invitrogen)
- 0.1M DTT (Invitrogen)
- Ribonuclease inhibitor, Cloned (Invitrogen)
- Hexamer (random primer) (Invitrogen)
- MMLV- reverse transcriptase (Invitrogen)
- 10mM dNTPs
- PCR tubes (Fisher Scientific)
- iTaq SYBR® Green (BIO-RAD)
- 96 well optical reaction plate with barcode (ABI PRISM, Applied Biosystems)
- MicroAmp™ Optical adhesive film (Applied Biosystems)

2.5 Quantitative Real Time PCR

Quantitative real time PCR was employed to investigate if a successful knock down of Mig-6 had been achieved in our epithelial and endothelial cells and to quantitate expression of a number of molecular markers in mouse lung tissue.

2.5.i: Reverse Transcriptase PCR (RT-PCR)

Firstly the following was mixed in a tube: 2µg RNA sample, 1µl dNTP, 1µl random primer, water to a volume of 12µl. This mixture was heated to 65°C for five minutes and then quick

chilled on ice. The following mixture was prepared and added to the RNA/dNTP/random primer mix: 4µl 5x first strand buffer, 2µl DTT, 0.5µl RNase inhibitor, 1µl MMLV reverse transcriptase, 0.5µl water. The RT-PCR mix was put on a thermocycler (MJ Research) and the following conditions programmed: 25°C 10 mins, 37°C 50 mins, 70°C 15 mins.

This cDNA was stored at -20°C until its use as the template for quantitative real time PCR.

2.5.ii: Quantitative Real-time PCR

Quantitative real-time PCR was performed by using Taqman probe or SYBR Green master mix (Applied Biosystems, Foster City, CA) to quantitate the expression levels of *Mig-6*, surfactant associated protein C (*SP-C*), *Tl α*, and mucin 5 subtypes A and C (*MUC5AC*), in the *Mig-6*^{+/+}, *Mig-6*^{-/-}, *Mig-6*^{f/f} and *Mig-6*^{d/d} mouse lungs. Primers and probe sequences are listed in **Table 2.1**.

cDNA samples were diluted 1 in 5 in DEPC water for *Mig-6*, *SP-C*, *Tl α* and *MUC5AC* and a further 1 in 500 for the 18S samples (This follows a protocol already in use in our lab). Once samples were diluted appropriately the following mixtures were prepared for each marker being investigated: cDNA 5µl, master mix (containing taq, forward and reverse primers, MgCl₂ and dNTPS) 1µl, H₂O 6.5µl. Reactions were prepared in 96 well optical reaction plates (Applied Biosystems) and the plates sealed with adhesive film to prevent evaporation during the reaction. Thermal conditions for the reaction were as follows: 50°C 2mins followed by 40 cycles of 95°C for 15seconds and 60°C for 1 minute. Data was collected at each 60°C point in the reaction. Levels for each target marker were compared for samples from *Mig-6*^{+/+}, *Mig-6*^{-/-}, *Mig-6*^{f/f} and *Mig-6*^{d/d} mice.

Table 2.1: Primer sequences for real-time PCR^a

<i>SP-C</i>	Forward: 5'-ACGACGACCACGAATTCCTG-3'
	Reverse: 5'-CCTCCCAACTACATGGTGGTG-3'
<i>Tlα</i>	Forward: 5'-TCAAAGCATCTGCCTTTGGAA-3'
	Reverse: 5'-ACTGTCTTGGCTTTGCTCCATT-3'
<i>MUC-5AC^b</i>	Forward: 5'- AGAATATCTTTCAGGACCCCTGCT -3'
	Reverse: 5'- ACACCAGTGCTGAGCATACTTTT -3'
	Probe: 5'- CTCAGCGTGGAGAATG -3'

^a Taqman primers and probes from Applied Biosystem (Foster City, CA) were used for quantification of gene *Mig-6*, *CC10*, and *18S rRNA* and the sequences are not listed as they are not available

^b Primers and probe of *MUC-5AC* were kindly provided by Dr. Christopher M. Evans from University of Texas, M.D. Anderson Cancer Centre.

2.6: Measurement of Alveolar Spaces:

Materials

- Images of H&E stained tissues taken at 40x magnification
- Grid
- Ruler

The size of alveolar spaces were measured on sections taken from wild type, *Mig-6* knock out, f/f and d/d mice in order to assess whether any difference in size is seen in the different mice. It has previously been seen in our lab that *Mig-6* knockout mice have larger alveolar

spaces than wild type mice so we wanted to see if the same was true in our induced knockout mice.

Measurements were performed on wild type, Mig-6 knock out, f/f and d/d mice. The size of the alveolar airspace was determined by measuring mean chord lengths on H&E-stained lung sections (59). Images were taken at 40x from five representative, non-overlapping fields of lung from at least 8 mice. A grid consisting of 6 black lines at 35- μ m intervals (scale) was overlaid on the image. Areas of bronchiolar airways and blood vessels were eliminated from the analysis. The length of lines overlapping the alveoli was measured and averaged giving the mean chord length of the alveolar space. All quantitative studies were performed blind with regard to animal genotype and were repeated by a second person to ensure no bias.

2.7: MTT Assay

Materials:

- dye solution (Promega)
- Solubilisation/stop solution (Promega)
 - N,N-dimethylformamide
 - Sodium dodecyl sulphate
 - Acetic acid
- UV spectrometer
- Cell titre plate

2.7 MTT Assay

We carried out MTT assays on our siRNA treated H441 and HMVEC cells to see if the knock down of Mig-6 had any effect on cell viability.

The MTT assay is a cell viability assay in which cell permeable **MTT** (3-(4,5-Dimethylthiazol-2-yl)-2,5-diphenyltetrazolium bromide), usually a yellow colour is reduced to purple formazan precipitate in living cells. Since the enzymes (reductases) that catalyse formazan formation from MTT are only active in living cells, the amount of formazan formed can be used as a measure of cell viability. Since formazan is insoluble in water, a solubilisation solution containing DMFO, SDS and Acetic acid is used to dissolve the formazan prior to measuring the absorbance at 570nm. MTT assays were performed on siRNA treated H441 and HMVEC-L in 24-well plates following standard protocols as a measure of cell viability following siRNA treatment. Following siRNA treatment, 75 µl of dye solution (Promega, Madison, MI) was directly added to each well. After incubation at 37°C for 4 hours, 500 µl of solubilisation solution (Promega) was added and mixed well. Absorbances at 570nm of the contents of the well were recorded and levels compared between siRNA treated and untreated cells.

2.8: Analysis of H441 cell line for mutated *Mig-6*

Materials:

- TOPO TA cloning kit (Invitrogen)
- OneShot *E.coli* cells (Invitrogen)
- LB Broth from LB broth base powder (Invitrogen)
- LB agar plates from LB agar powder (Invitrogen)
- X-gal (Invitrogen)
- Ampicillin (Invitrogen)
- Agarose (Fisher Scientific)
- 5x TBE
 - o 53g Tris base (Fisher Scientific)
 - o 27.5g boric acid (Fisher Scientific)
 - o 20ml of 0.5M EDTA (Fisher Scientific)
 - o Make up to 1L with water
- Blue loading dye (Promega)
- 0.5mg/ml Ethidium bromide (Sigma)
- Power supply
- Agarose gel electrophoresis tank
- Microwave
- Conical flask
- 10x high fidelity PCR buffer (Invitrogen)
- dNTP mix (Invitrogen)
- 50mM MgCl₂ (Invitrogen)
- Primers:

- Mig-6 code F&R (Invitrogen)
 - Mig-6 code UTR F&R (Invitrogen)
- Platinum high fidelity Taq (Invitrogen)
- QIAprep Miniprep kit (QIAGEN)
- Microcentrifuge
- Microcentrifuge tubes
- Tubes for LB broth
- SOC medium (Invitrogen)
- Peltier thermal cycler (MJ Research)
- 1kb DNA ladder (New England Biolabs)
- EcoR1 restriction enzyme (Invitrogen)
- EcoR1 restriction buffer (Invitrogen)
- UV spectrometer

2.8: Analysis of H441 cell line for mutated *Mig-6*

We decided to sequence the Mig-6 gene in the H441 cell line we were using to ensure that it contained no mutations. If the H441 was found to be mutated we wouldn't be able to use it for Mig-6 functional studies. To determine whether H441 cells carried a mutated Mig-6 allele, we performed a cloning reaction and sequenced all the products.

The cells were grown to a confluency of ~70% in the tissue culture core at Baylor College of Medicine. RNA was isolated from cells and quantified as described in section 2.4. Isolated RNA was reverse transcribed to cDNA as detailed in section 2.5.

2.8.1: *Mig-6* PCR:

The cDNA was used as a template for amplification of the *Mig-6* gene. Reaction volume was 50µl which was made up of the following components: 5µl 10x high fidelity PCR buffer, 1µl 10mM dNTP mix, 2µl 50mM MgCl₂, 0.2µl Platinum Taq High Fidelity, 0.5µl forward primer (10µM), 0.5µl reverse primer (10µM), 3µl template DNA and 37.8µl water.

All primer sequences used in this experiment were designed using Vector NT1 Advance 10 software from Invitrogen. Primers were synthesised by Invitrogen and sequences are shown in **Table 2.2**. Gene amplification consisted of an initial denaturation step where reaction mixtures were incubated at 94°C for 2mins. This was followed by 30 cycles of denaturation at 94°C for 30 seconds, annealing at 55°C for 30 seconds and extension at 68°C for 2 minutes. All amplifications were carried out in a Peltier thermal cycler (MJ Research)

Primer	Sequence 5'-3'	Product Size (bp)	Annealing Temperature	Magnesium concentration
Mig-6 Code F	ATGTCAATAGCAGGAGTTGC	1386	55°C	5mM
Mig-6 Code R	CTAAGGAGAAACCACATAGGAT			5mM
Mig-6 Code UTR F	ACAGGTTTGGAGATGTCCCA	1466	55°C	5mM
Mig-6 Code UTR R	GAGAACCATTGCTCCTATG			5mM

Table 2.2: Primer sequences, amplicon size, MgCl₂ concentration and annealing temperature for Mig-6 PCR reactions.

Amplicons were visualised following electrophoresis using a 1% (w/v) agarose gel stained with ethidium bromide (0.5 µg/ml) in a 1 X Tris-Borate-EDTA (TBE) buffer. A 1kb DNA ladder (New England Biolabs) was run alongside the samples in order to determine amplicon size. The gel was run at a constant voltage (100V) until the bands had migrated about 1/2 to 2/3 of the distance to the end of the gel. The resulting bands (~1.4kb) were visualised and then cut out (in order to gel purify the DNA).

Making the 1% agarose gel:

1g of low melting point agarose powder was dissolved in 100ml of 1X TBE buffer in a conical flask and microwaved for approximately 90 seconds. When it was determined that the agarose was fully dissolved, the flask was allowed to cool to ~60°C. Once the mixture had cooled, 50µl of ethidium bromide was added and the flask swirled to mix. The agarose was poured into the gel mould and allowed to set. Prior to loading, the comb was removed. Samples were prepared for loading by the addition of 10µl of 5x loading dye to a 50µl sample volume. The entire volume was loaded onto the gel alongside the 1kb ladder.

2.8.2 DNA Purification from agarose gel:

DNA was purified using the QIAEX II gel extraction kit from QIAGEN as follows: the band was cut from the gel using a blade and its weight recorded (this determines how much of the buffers to add in the purification process). The gel was dissolved in 450µl QX buffer and 15µl of resin was added. The mixture was vortexed and placed on a heating block at 40-50°C for a total of ten minutes, vortexing the sample every two minutes. The sample was centrifuged for ~15 seconds to pellet the resin, the supernatant was removed, 500µl of fresh buffer was added and the mixture vortexed to resuspend the resin. Sample was centrifuged to pellet the resin followed by adding 500µl of wash buffer, vortexing to resuspend the pellet and centrifugation (~15 seconds). This wash step was then repeated. Following the second

wash step, the supernatant was removed and the pellet air dried at room temperature until most of the resin had turned white. 15µl of deionised water was added, the sample vortexed and then incubated at 50°C for five minutes. Sample was centrifuged to pellet and entire supernatant was transferred to a fresh tube. This purified DNA was used for the TOPO® cloning reaction.

2.8.3 TOPO® Cloning Reaction

The following reaction mixture was prepared: 2µl of gel purified DNA, 1µl salt solution (from the TOPO TA cloning kit), 2µl sterile deionised water and 1µl of TOPO vector containing DNA ligase. The mixture was incubated for five minutes at room temperature and then placed on ice in preparation for the transformation reaction.

Transformation procedure:

One vial of One Shot *E. coli* cells per transformation were thawed out. 2µl of the TOPO cloning mixture prepared above was added to the *E. coli* and mixed. The reaction was incubated on ice for 30 minutes followed by heat shock for 30-45 seconds at 42°C. 250µl of room temperature S.O.C medium was added to the cells. This was incubated at 37°C for one hour with shaking for the duration. 50µl of the transformation reaction was spread onto pre-warmed LB agar plates containing x-gal and 100µg/ml ampicillin. Plates were incubated at 37°C overnight

2.8.4 Analysis of positive clones:

Following overnight culture, the LB plates were examined for evidence of positive clones (white colonies). A positive clone is one which has taken up the vector with our DNA inserted and hence the beta galactosidase gene in TOPO that ordinarily converts XGal into a blue product is disrupted. Tubes were prepared each containing 3ml of LB broth with 100µg/ml ampicillin. Using a pipette tip, one colony was picked off the plate and this tip put

into one of the tubes containing LB broth with ampicillin. The process was repeated for all tubes. The tubes were incubated at 37°C overnight with constant shaking.

2.8.5 Plasmid Isolation and DNA purification:

The overnight broth cultures were spun down to obtain a pellet of bacterial cells and the supernatant discarded. Plasmid DNA isolation purification was carried out using the QIAprep Miniprep kit from QIAGEN. The bacterial pellet was resuspended in 250µl of buffer P1 and transferred in a microcentrifuge tube. 250µl of buffer P2 was added and mixed by inverting 4-6 times. 350µl of buffer N3 was added and mixed by inversion (at this point the solution should become cloudy). Samples were centrifuged at 10,000 rpm for ten minutes. The supernatant was transferred to a QIAprep spin column. This was spun for ~60 seconds and the flow through discarded. To wash the sample, 750µl of buffer PB was added and the tubes spun at 13,000 rpm for 60 seconds. The flow through was once again discarded and tubes centrifuged for a further 60 seconds. The column was placed into a microcentrifuge tube and 50µl of buffer EB was added, left to stand at room temperature for one minute and then centrifuged for one minute to elute the DNA. The DNA was quantified by UV spectrometry (OD_{260nm}:OD_{280nm}) and then three samples were sent for sequence analysis.

When a sequence result was received the sequence was compared to the known Mig-6 gene sequence to see whether any mutations were present in the sequence from our H441 cells.

2.8.6 EcoRI digestion of plasmid:

Prior to sending the samples for sequence analysis, an EcoRI digestion was carried out to ensure that the correct insert was present. 2µl of plasmid DNA, 0.5µl EcoRI, 1µl of buffer 3 and 6.5µl were mixed in a tube and incubated at 37°C for one hour. The samples were then run on a 1% agarose gel and resulting bands were visualised on a UV transilluminator. For samples with the correct insert present there were 3 different bands present (the Mig-6

sequence itself has an EcoRI site which is cut) bands are present at 4kb (the vector), 1kb and 0.5kb (the insert).

3. Results

To obtain our Mig-6^{d/d} mice, *Rosa26-Cre-ERT2* mice were crossed with *Mig-6^{flox/flox}* (*Mig-6^{ff}*) mice and the resulting *Rosa26-Cre-ERT2; Mig-6^{flox/flox}* (*Mig-6^{d/d}*) or *Mig-6^{ff}* mice (2 months old) were injected peritoneally with 1 mg of Tamoxifen for 5 days. These mice were further maintained for 4 months before analysis. At six months old mice were sacrificed, lung tissue harvested, mRNA extracted and real time quantitative PCR for Mig-6 was carried out using 18s RNA as a control.

3.1 Real time PCR to show knock-out of Mig-6 in Mig-6^{-/-} mice and induced knock-out of Mig-6 in Tamoxifen treated Cre⁺ d/d mice

The aim of this experiment was to test whether the Tamoxifen treatment had been successful in inducing the knockout of Mig-6 in the Cre⁺ (*Mig-6^{d/d}*) mice. We already know from previous experiments in our lab that Mig-6 is involved at the developmental stages of the lung (5) but we wanted to investigate what role, if any, Mig-6 has at the adult stage. The administration of Tamoxifen to *Mig-6^{ff}* and *Mig-6^{d/d}* mice at 2 months old is the first stage in the process, if the Tamoxifen treatment is successful in knocking out Mig-6 in the Cre⁺ mice then we can study Mig-6 in the adult mouse. As a large proportion of *Mig-6^{-/-}* mice die before reaching adulthood it is difficult to investigate Mig-6 beyond the neonatal period. Cre-ERT is a functional Tamoxifen-dependent recombinase in cultured cells and transgenic mice. By controlling the time point at which the target gene is excised using an inducible Cre recombinase, it allows us to look at the role of the gene later in the developmental process or in adult life as well as allowing tissue specific excision of the gene of interest (26).

The figure 3.1 below shows the relative expression of Mig-6 mRNA in our transgenic Tamoxifen treated mice compared to a wild type strain.

Significant differences were noted between the wild type mice and the knockout (-/-) mice as well as the Tamoxifen treated Cre⁺ (d/d) mice. The Tamoxifen treated Cre⁻ (f/f) mice had Mig-6 levels significantly different to the knockout (-/-) and induced knockout mice. Statistics were performed using One Way ANOVA with a Bonferroni post hoc test, (*p<0.05).

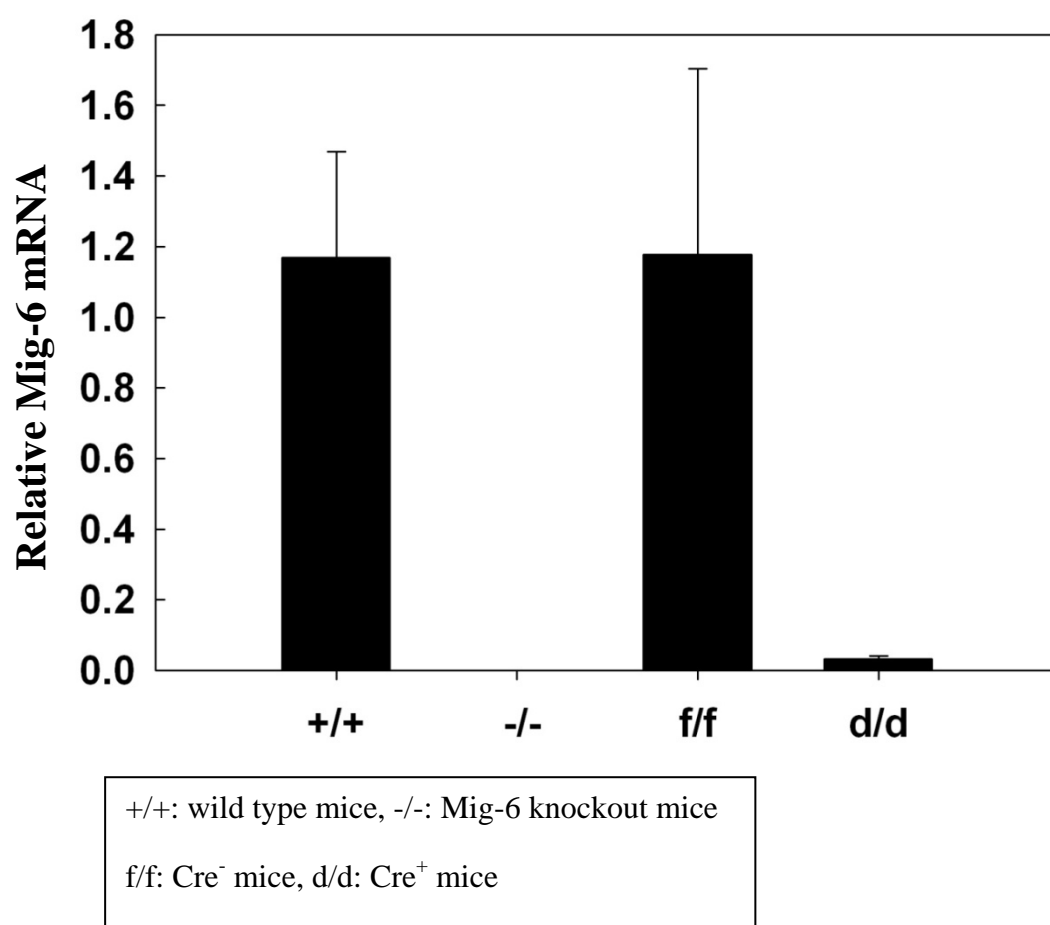


Figure 3.1: Quantitative real time PCR analysis of mRNA levels isolated from 6 month old Mig-6^{+/+}, Mig-6^{-/-}, Mig-6^{f/f} and Mig-6^{d/d} lungs for expression of Mig-6

Once we successfully knocked out Mig-6 in these adult mice the next step was to carry out a number of experiments looking at: General lung morphology, molecular markers, size of alveolar spaces, sacrificing mice at different time points following the knockout of Mig-6.

3.2 Comparison of the morphology of Mig-6^{f/f} and Mig-6^{d/d} adult mouse lungs

Mig-6 plays a role in lung development, highlighted by altered lung morphology/reduced airway space in Mig-6^{-/-} mice (5). We investigated whether lung morphology is altered when Mig-6 is deleted in adult mice. To do this, we examined whether morphological differences would be observed between the Mig-6^{f/f} and Mig-6^{d/d} mice. Mice were sacrificed at approximately six months of age and the lung tissue harvested. This tissue was processed to wax blocks in preparation for sectioning and staining. 4µm sections were cut using a microtome and stained using a haematoxylin and eosin stain to show general morphology. The H&E staining method involves application of the basic dye haematoxylin, which colours basophilic structures with blue-purple hue, and alcohol-based acidic eosin, which colours eosinophilic structures bright pink.

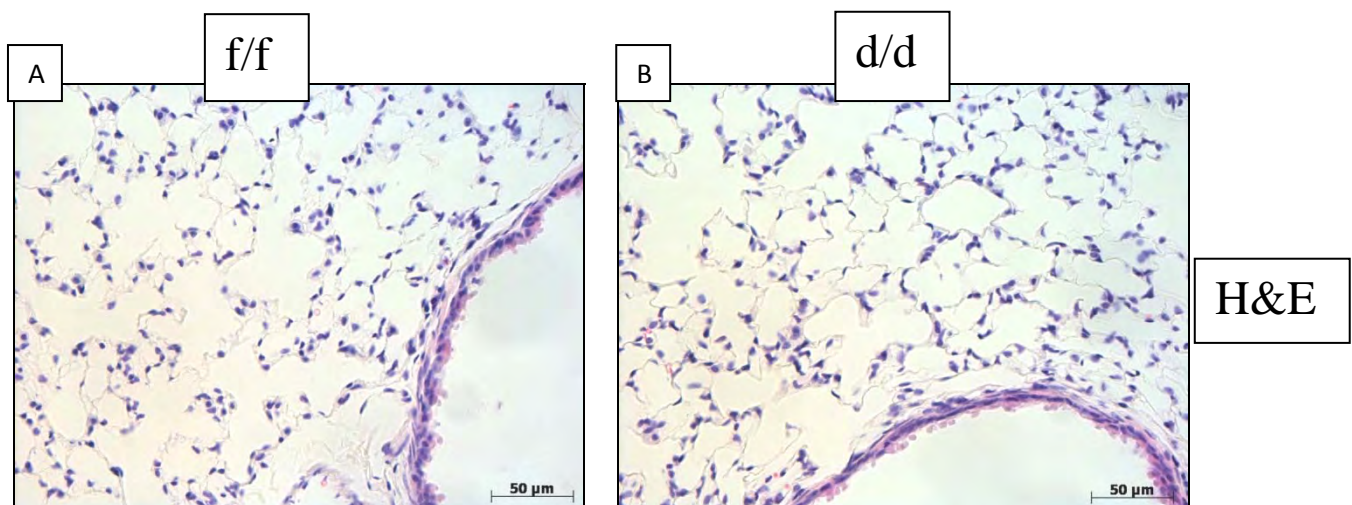


Figure 3.2

Panels A&B above show representative H&E stained lung sections from adult Mig-6^{f/f} and Mig-6^{d/d} mice.

No morphological differences were observed between adult lungs obtained from Mig-6^{f/f} and Mig-6^{d/d} mice upon H&E staining. As the lungs were fully formed in the adult mice before

Mig-6 was knocked out it would seem that Mig-6 does not have any noticeable effect on lung morphology after the initial development stage.

3.3 Adult Mig-6^{f/f} and Mig-6^{d/d} mice have normal airspaces

The next step after a general assessment of morphology of the lung sections by staining was to take a series of sections stained using H&E to measure the size of the airspaces in our RosaCreERT2 x Mig-6^{f/f} mice. For comparison purposes we also measured sections from wild type (Mig-6^{+/+}) and Mig6 knock out (Mig-6^{-/-}) mice. It has previously been shown in our lab that Mig-6^{-/-} mice have larger airspaces than Mig-6^{+/+} mice (5). We wanted to examine our induced knock out (Mig-6^{d/d}) mice to see if there was any effect on size of airspace. All measurements were performed blind with respect to animal genotype.

Mig-6^{+/+} and Mig-6^{-/-} measurements were in line with previous results from our lab and showed that Mig-6^{-/-} mice have significantly larger airspaces than wild type (Mig-6^{+/+}) mice. This indicates a role for Mig-6 in either the development of or maintenance of airspaces in lung. Interestingly, a significant difference in size was noted between the Mig-6^{-/-} mice and all other genotypes examined, including our induced Mig-6 knockout model (Mig-6^{d/d}). This is strongly indicative that Mig-6 plays an important role in lung development but expression of Mig-6 in the adult lung does not affect airway size. In line with this hypothesis, no significant difference was noted between Mig-6^{+/+}, Mig-6^{f/f} or Mig-6^{d/d} mice. Statistics were performed using One Way ANOVA with a Bonferroni post hoc test (*p<0.05).

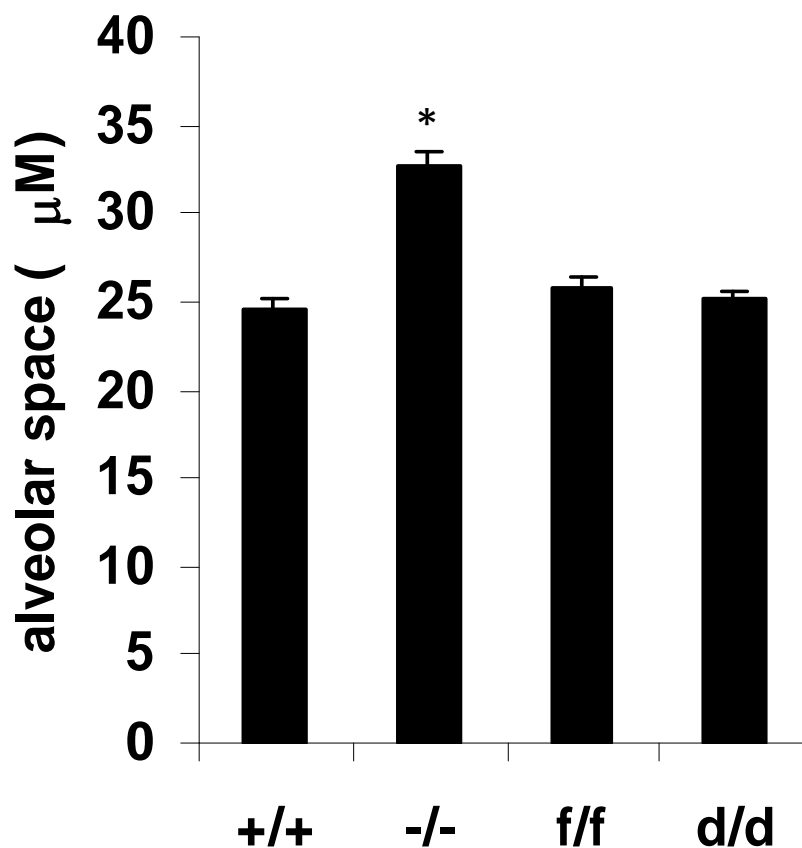


Fig 3.3. Alveolar space measurements were carried out on wild type (Mig-6^{+/+}) and knock out (Mig-6^{-/-}) mice as well as Tamoxifen treated Cre⁻ (Mig-6^{f/f}) and Cre⁺ (Mig-6^{d/d}) mice. Mig-6^{-/-} mice have significantly increased airspaces while the Tamoxifen treated mice (both Mig-6^{f/f} and Mig-6^{d/d}) have airspaces in line with wild type measurements (n=8).

3.4 Expression of Pulmonary Epithelial Cell markers in Mig-6^{-/-} vs. Mig-6^{+/+}

After measurement of the alveolar spaces in our mice we found no difference at the morphological level. It was decided to then look at a number of different molecular markers to investigate whether any differences would be apparent at the molecular level of the lung epithelium in our Mig-6^{f/f} vs., Mig-6^{d/d} mice since there are noted differences between wild type and Mig-6^{-/-} mice.

RNA was isolated from the lungs of wild type and Mig-6^{-/-} mice in addition to the Mig-6^{f/f} and Mig-6^{d/d} mice and the levels of the following molecular markers analysed using real time PCR CCSP, T1 alpha, Muc5ac and SP-C. We analysed the marker levels in wild type and knockout mice alongside our Tamoxifen treated mice (f/f and d/d). Although we observed no phenotypic change in the Mig-6^{d/d} mice we could not assume there would be no change at the molecular level following the deletion of Mig-6 in adult mice so we investigated the molecular markers.

3.4.1 CCSP levels in Mig-6^{+/+}, Mig-6^{-/-}, Mig-6^{f/f} and Mig-6^{d/d} mice

CCSP is Clara cell secretory protein and a significant difference is seen between Mig-6^{+/+} and Mig-6^{-/-} mice (5). CCSP is a protective lung protein which is believed to have antioxidant, immunomodulatory and anticarcinogenic properties (60). CCSP is a developmental marker involved in cellular differentiation in respiratory epithelium during development and early life (61). Mig-6^{-/-} mice have decreased CCSP levels (5).

Statistics were carried out on the data using One Way ANOVA with a Bonferroni post hoc test, *p<0.05. Sample size was between five and nine mice for each group (n=5-9). We found that there was a significant difference in the CCSP levels measured between our Mig-6^{f/f} and Mig-6^{d/d} mice after deletion of Mig-6 with the treatment of Tamoxifen. Despite the high variability between samples, this assay had sufficient numbers to show a significant decrease in CCSP expression in Mig-6^{d/d} mice compared with Mig-6^{f/f} controls

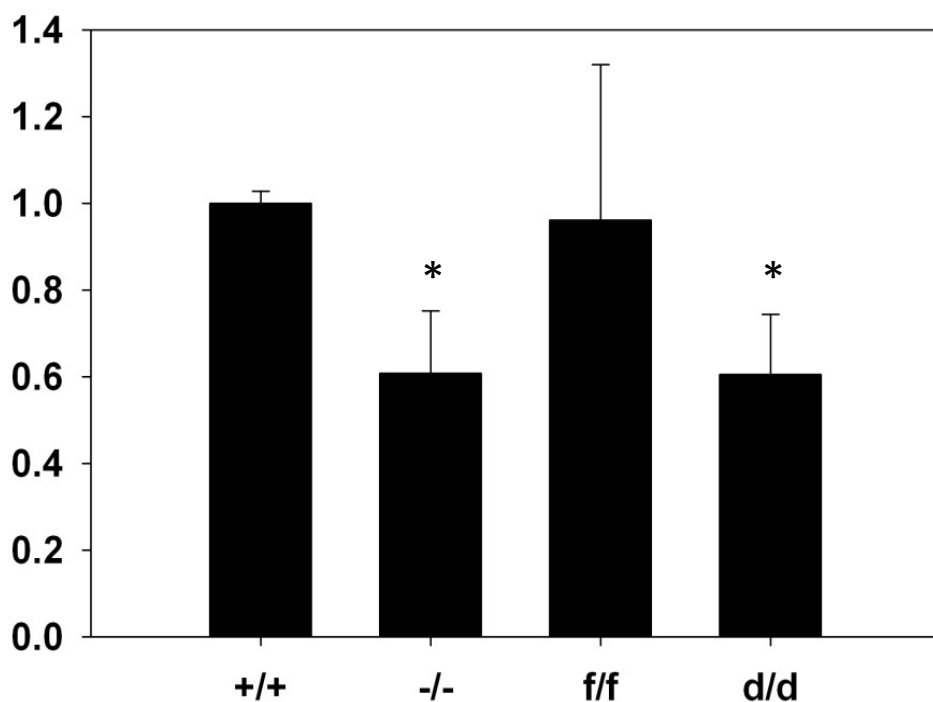


Figure 3.4: Quantitative real-time PCR analysis of mRNA levels isolated from adult *Mig-6*^{+/+}, *Mig-6*^{-/-}, *Mig-6*^{f/f} and *Mig-6*^{d/d} lungs for the expression of Clara cell secretory protein (CCSP)

3.4.2 T1 Alpha levels in *Mig-6*^{+/+}, *Mig-6*^{-/-}, *Mig-6*^{f/f} and *Mig-6*^{d/d} mice

T1 alpha levels increase in the lung throughout foetal development and is the first marker gene known to be expressed in the adult lung solely by the alveolar type I epithelial cell (62). As *Mig-6* levels also increase and decrease at various stages in lung development we thought it would be interesting to look at T1 alpha levels in our different mouse populations to see whether the absence or presence of *Mig-6* impacted on the level of T1 alpha present.

There is a significant difference in T1 alpha levels between *Mig-6*^{+/+} and *Mig-6*^{-/-} mice with *Mig-6*^{-/-} having greatly reduced amounts compared with the wild type control. No significant difference in T1 alpha was measured between *f/f* and *d/d* mice, nor did T1 alpha levels in

these mice differ from the wild type levels measured. This is an interesting result to note as T1 alpha levels were not affected when Mig-6 is knocked out at the adult stage of life while if it is knocked out in the germline then the resulting Mig-6^{-/-} mice. This would suggest that Mig-6 and T1 alpha expression are both linked within the developmental process but expression of T1 alpha is independent of expression of Mig-6 in fully developed adult lungs.

Statistics were performed using One Way ANOVA with a Bonferroni post hoc test, *p<0.05 (n=5-9).

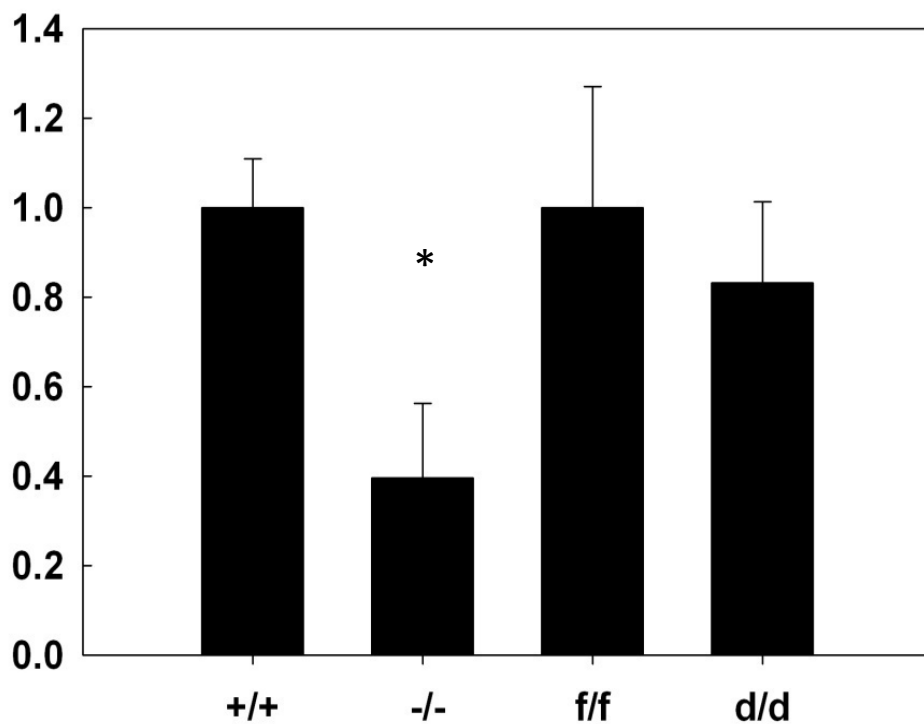


Figure 3.5: Quantitative real-time PCR analysis of mRNA levels isolated from adult *Mig-6*^{+/+}, *Mig-6*^{-/-}, *Mig-6*^{f/f} and *Mig-6*^{d/d} lungs for the expression of T1 alpha

3.4.3 SP-C levels in Mig-6^{+/+}, Mig-6^{-/-}, Mig-6^{f/f} and Mig-6^{d/d} mice

SP-C is surfactant protein C and is found solely in the surfactant layer of the alveoli (63). It has been reported to have the following three functions:

1: catalyze the formation of surface-associated three-dimensional structures at the air-liquid Interface, 2: assist in the transfer of lipids from the monolayer to form stacked multi-layer structures, and 3: act as protection against surfactant inactivation by serum proteins (64). Mechanical strain has been shown to increase SP-C levels (65).

SP-C levels were analysed in our different transgenic mice and control wild type mice- Mig-6^{+/+}, Mig-6^{-/-}, Mig-6^{f/f} and Mig-6^{d/d}. The only significant difference noted was between the Mig-6^{-/-} mice and all three other genotypes. Because the only difference in SP-C levels was seen in mice where Mig-6 is knocked out prior to foetal development this may point to a link between Mig-6 and SP-C in the developmental stages of life. It may be that Mig-6 has a regulatory role and prevents overexpression of SP-C during development and when this control is removed SP-C levels increase greatly. Alternatively, in the absence of Mig-6 expression the alveolar structures are under greater mechanical strain and that this may indirectly lead to elevated SP-C expression. As there was no significant change in SP-C when Mig-6 is knocked out post development it would appear that whatever role Mig-6 plays in controlling SP-C levels is present only early in life.

Statistics were performed using One Way ANOVA with a Bonferroni post hoc test,

*p<0.05(n=5-9).

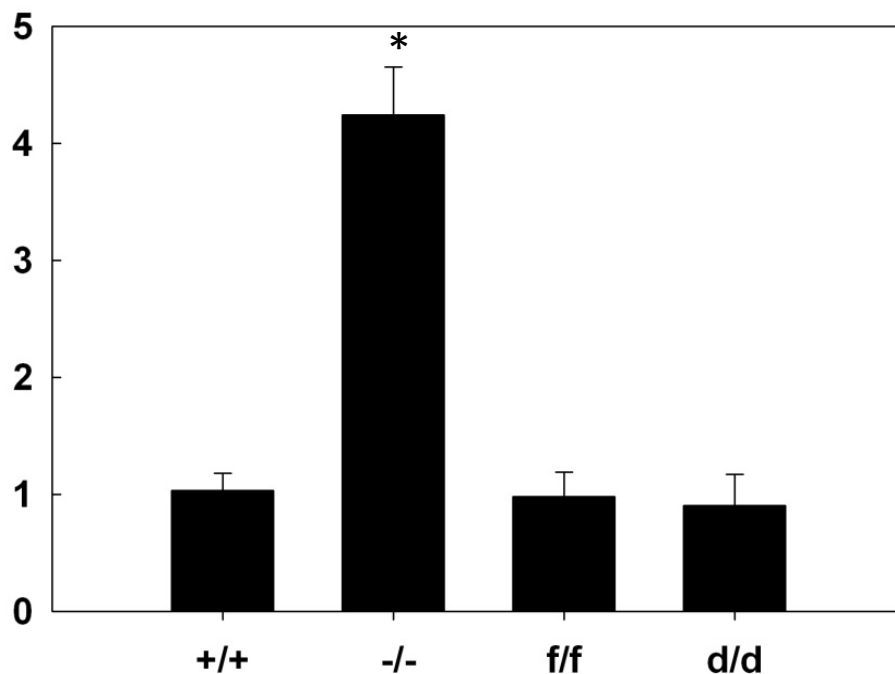


Figure 3.6: Quantitative real-time PCR analysis of mRNA levels isolated from adult *Mig-6*^{+/+}, *Mig-6*^{-/-}, *Mig-6*^{f/f} and *Mig-6*^{d/d} lungs for the expression of surfactant protein C (SP-C)

3.4.4 MUC5AC levels in *Mig-6*^{+/+}, *Mig-6*^{-/-}, *Mig-6*^{f/f} and *Mig-6*^{d/d} mice

MUC5AC is a gel-forming glycoprotein of gastric and respiratory tract epithelia that protects the mucosa from infection and chemical damage by binding to inhaled microorganisms and particles that are subsequently removed by the muco-ciliary system (66). Hypersecretion of mucins including MUC5AC is seen in many airway diseases and results in impairment of muco-ciliary clearance and bacterial super infection (67).

In our measurements we found that wild type mice have low levels of mucin MUC5AC but in knockout mice (*Mig-6*^{-/-}) there is a dramatic increase in MUC5AC levels. The Tamoxifen

treated $Mig-6^{d/d}$ and $Mig-6^{f/f}$ mice had MUC5AC levels similar to those of the wild type mice. As levels of this mucin were not altered when $Mig-6$ was knocked out in the adult phase of life it would appear that the lungs of $Mig-6^{d/d}$ mice are phenotypically normal and not subject to excessive airway diseases (these results are for unchallenged mice). Statistics were performed using One Way ANOVA with a Bonferroni post hoc test, $*p<0.05$ ($n=5-9$).

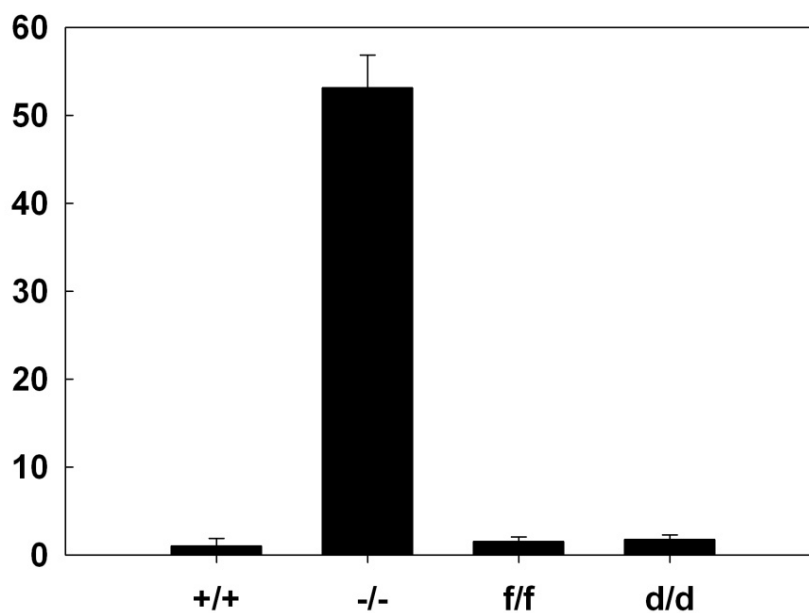


Figure 3.7: Quantitative real-time PCR analysis of mRNA levels isolated from adult $Mig-6^{+/+}$, $Mig-6^{-/-}$, $Mig-6^{f/f}$ and $Mig-6^{d/d}$ lungs for the expression of mucin 5AC (MUC5AC)

Overall result from measurement of molecular markers: in all cases there was a significant difference in levels between wild type and knockout mice. The induced knockout mice had similar levels of expression of MUC5AC, SP-C and T1alpha while CCSP levels in $Mig-6^{d/d}$ mice were significantly different to wild type mice and $Mig-6^{f/f}$ controls.

Knocking out Mig-6 in adult mice appears to have had no effect on phenotype or the majority of molecular markers for normal lung function. This would suggest that the lungs in adult Mig-6^{d/d} mice are essentially normal even when Mig-6 expression is ablated using Tamoxifen although our results indicate that CCSP expression moderately decreases in Mig6d/d mice that are indicative of minor lung abnormalities or dysfunction. Therefore it appears that Mig-6 exerts greater influence during the developmental stage of the lung. As Mig-6 is a stress induced gene it may also be important in the lung's response to damage/hypoxia/other injury, in these cases we would hypothesise that a re-emergence of developmental pathways could occur.

3.5 Silencing of Mig-6 expression in H441 epithelial lung cells using RNA interference.

The fact that Mig-6 is expressed in adult lungs points to the conclusion that it must serve some purpose in adult mice but our results indicate that it does not appear to play a major role in lung morphology or lung function. In order to look at the potential role(s) Mig-6 might play in adult mice we used lung cell lines to investigate the effect of knocking down Mig-6 expression in different cell types (both epithelial and endothelial cells).

We decided to look at Mig-6 expression and function specifically in epithelial cells so we used the H441 epithelial cell line for this purpose. The pulmonary epithelium plays a vital role in the body through its role in gaseous exchange ensuring a constant supply of oxygen is available to all cells throughout the body. In addition to its role in gaseous exchange the pulmonary epithelium also has a number of other roles: It provides a protective barrier between the host and the outside environment, contributes to the maintenance of lung fluid balance, plays a role in the metabolism of endogenous mediators (68) and is capable of regeneration, allowing normal cell turnover and restoration of airway and alveolar functions after lung injury (69). Lung epithelium produces surfactant and several proteins which are

important as part of the immune defences of the body (14). Because of these roles we were interested in investigating what effect (if any) silencing Mig-6 expression in this specific cell type would have.

These experiments would provide an *in vitro* model to investigate the role of Mig-6 in epithelial cells. Half of our cells would be treated with siRNA with the other half treated with a control siRNA that does not silence any known gene. Successful silencing of Mig-6 expression in the treated cells would allow us to harvest RNA and proteins from these cells to examine what effects silencing of Mig-6 had on downstream elements of the signalling pathway and thus gain further insight into what role Mig-6 has in adult lung epithelial cells.

The first step in looking at the role of Mig-6 in epithelial cells was to use siRNA to knock down Mig-6. Previous experiments carried out in my lab using different concentrations of siRNA showed 50nm to be a sufficient concentration to silence Mig-6 expression. Following successful knock down of Mig-6 in this cell type the goal was to look at various elements of downstream signalling pathways to see if removing Mig-6 has an effect. Mig-6 is a known negative regulator of EGFR (70, 71) so we chose to look initially at signalling from the EGFR.

The graph below (figure 3.8) shows the result of real time quantitative PCR (qPCR) analysis on our siRNA treated and untreated H441 epithelial cells. RNA was extracted from the cells as detailed in the Methods (section 2.4) and converted to mRNA. Real time PCR was carried out for Mig-6 levels with 18s ribosomal RNA as a control. Significant difference was noted in Mig-6 expression when cells were treated with Mig-6 siRNA compared with cells treated with either no siRNA or siControl. No significant difference was noted between the cells treated with siControl and the cells not treated with siRNA indicating that the decrease in Mig-6 expression was due to the specific RNA interference activity of our siRNA. The

success of this experiment allowed us to continue our experiments and look at the effect that this silencing of Mig-6 has on elements of the EGF signalling pathway.

Statistics were performed using One Way ANOVA with a Bonferroni post hoc test, ($p < 0.05$).

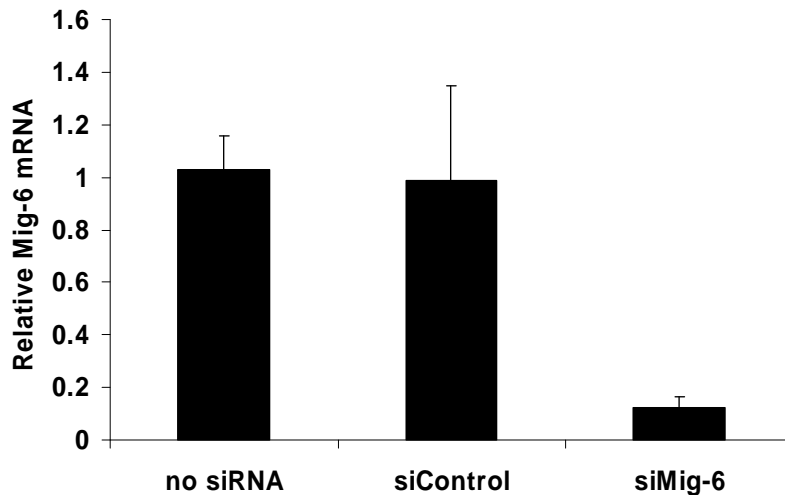


Figure 3.8: Real time quantitative PCR to show successful knock-down of Mig-6 in H441 cells using 50nm siRNA

3.6 Silencing Mig-6 expression in HMVEC endothelial lung cells using RNA interference

Endothelial cells play an important role in the lung as the cells which line the capillaries that surround the alveoli in a network of blood vessels. As branching of the airways occurs in the developmental stages each new bud is surrounded by a network of endothelial cells. It is likely that Mig-6 also plays a role in regulating endothelial lung cell function; therefore we chose to look at the role of Mig-6 in endothelial cells using the Human Microvascular Endothelial Cells (HMVEC) cell line as our model.

The aim was to successfully silence Mig-6 in HMVEC cells using the same method as for the epithelial cells. We planned to measure the same elements of the signalling pathway as in the

epithelial cells and see if there were any similarities or differences in the effect knocking down Mig-6 has on epithelial cells vs. endothelial cells.

The graph below shows the result of real time quantitative PCR analysis on our siRNA treated and untreated endothelial cells. RNA was extracted from the cells as detailed in section 2.4 and converted to mRNA. Real time PCR was carried out for Mig-6 levels with 18s ribosomal RNA as a control. Significant difference was noted between the cells treated with Mig-6 siRNA and cells treated with either no siRNA or siControl. No significant difference was noted between the cells treated with siControl and the cells not treated with siRNA. Statistics were performed using One Way ANOVA with a Bonferroni post hoc test, $p < 0.05$.

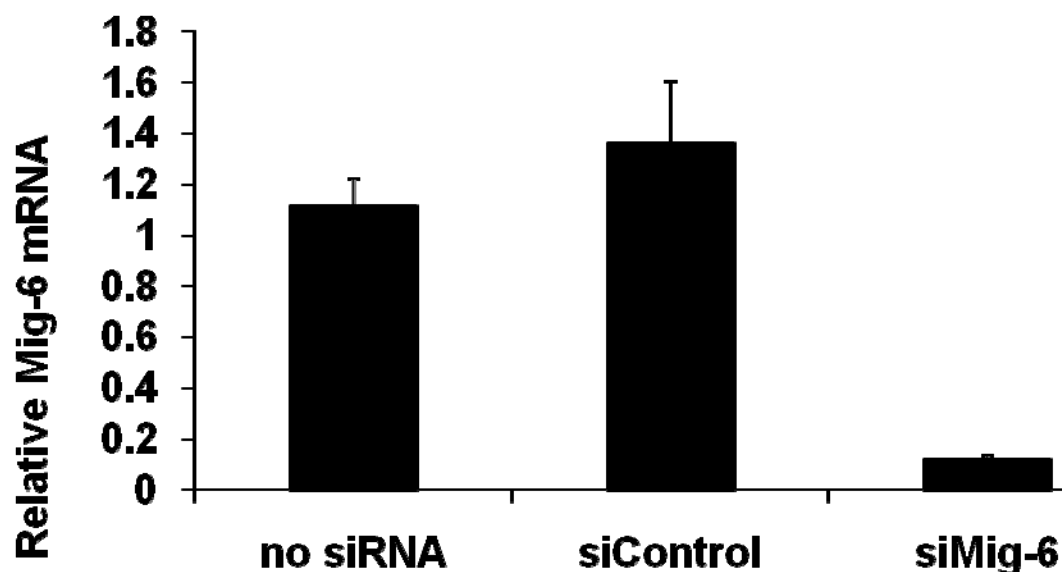


Figure 3.9: Real time quantitative PCR showing successful knockdown of Mig-6 in endothelial cells using 50nm siRNA. Levels of Mig-6 mRNA were compared in cells treated with control siRNA, Mig-6 siRNA and untreated cells.

3.7 Knockdown of Mig-6 leads to changes in cell proliferation: MTT assay

EGF signalling is involved in development of the lung and can activate downstream signalling, Ras-PI3K/Akt and Ras/MAPK and cross-talk with other growth factors such as TGF- β 1 and HGF signalling which are all important in lung development (5). As Mig-6 plays a role in the EGF signalling pathway it is plausible to hypothesise that if Mig-6 is altered or silenced it may have an effect on the cells in which we silenced Mig-6 expression and the function of Mig-6 in these cells might be established on the basis of silencing the expression of Mig-6 using RNA interference. Moreover, Mig-6 deletion affects lung morphology during development which may be regulated by increased cell proliferation / cell death due to Mig-6 expression.

We carried out a cell viability (MTT) assay to look at whether knocking down Mig-6 in our epithelial cells and endothelial cells has any effect on cell viability and if so would both cell types be affected in the same way or differently.

The MTT assay is a cell viability assay in which MTT (3-(4,5-Dimethylthiazol-2-yl)-2,5-diphenyltetrazolium bromide), usually a yellow colour is reduced to purple formazan in living cells. Since formazan is insoluble in water, a solubilisation solution containing DMFO, SDS and Acetic acid is used to dissolve the formazan prior to measuring the absorbance at 570nm. Since the enzymes (reductases) that catalyse formazan formation from MTT are only active in living cells, the amount of formazan formed can be used as a measure of living cells (72). By looking at this type of assay we can see in vitro how cellular proliferation is affected and get some idea of how different cell types would be affected by lack of Mig-6 in vivo. Increased numbers of viable cells may indicate increased proliferation while a decrease in viable cells may be an indication that knocking down Mig-6 leads to increased apoptosis or decreased cellular proliferation. Results in Figure 3.10 below show that following

knockdown of Mig-6 in the epithelial cells, there was a significant increase in the amount of viable cells present when the MTT assay was performed which may point to increased cellular proliferation or cell survival in this cell type. The opposite pattern was observed in the endothelial cells with significantly decreased numbers of viable cells present following knock down of Mig-6 by siRNA treatment. This may suggest that lack of Mig-6 in endothelial cells leads to increased apoptosis or decreased cellular proliferation.

Statistics were performed using One Way ANOVA with a Bonferroni post hoc test, * $p < 0.05$.

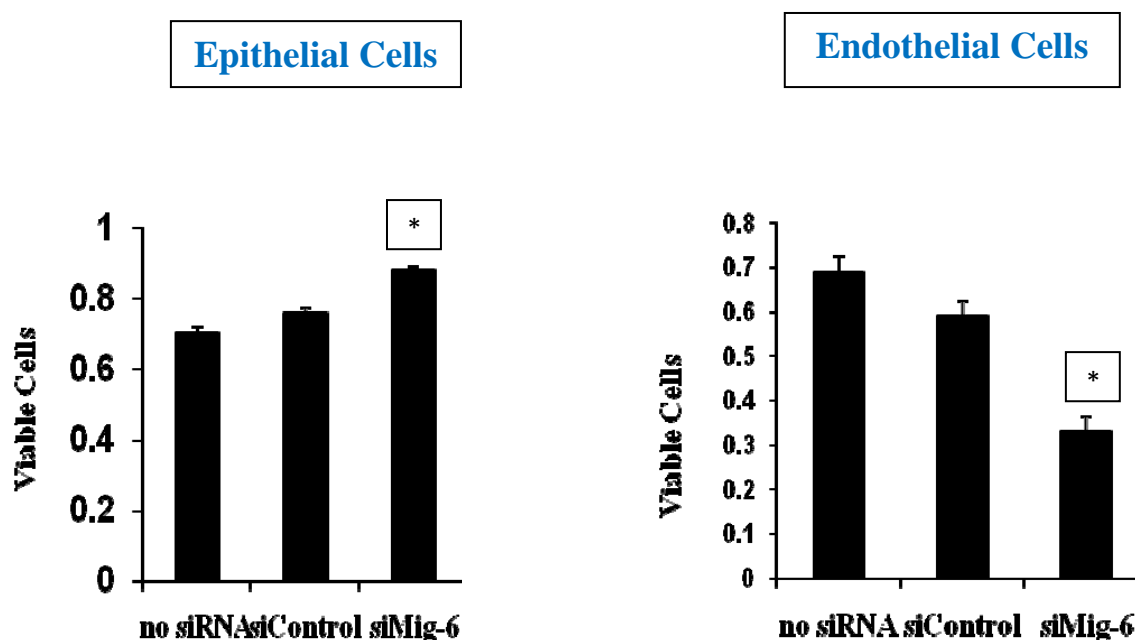


Figure 3.10: Results of MTT (cell viability) assay in H441 epithelial cells and HMVEC endothelial cells showing increased levels of viable epithelial cells and decreased levels of endothelial cells following treatment with 50nm siRNA

3.8 Analysis of H441 cell line for mutated *Mig-6*

To ensure that the H441 epithelial cell line we were using did not contain any mutations in its *Mig-6* gene, we chose to sequence *Mig-6* expressed by this cell line. It was important that no mutations were present as we were using this cell line for a large number of our experiments and should there be any mutations in its *Mig-6* then our data would prove to be compromised. To investigate our H441 cells we isolated RNA and amplified the *Mig-6* sequence using primers designed in house. We carried out a cloning reaction and sent the products for sequencing. Analysis of the sequencing results showed that no mutations were present in the *Mig-6* gene in our H441 cell line.

H441 cells were cultured and the RNA isolated once the cells were at ~70% confluency. RT-PCR was performed followed by *Mig-6* PCR. Two sets of primers were used in the *Mig-6* PCR- *Mig-6* code and *Mig-6* UTR. *Mig-6* code is used to amplify only the coding region of *Mig-6* while *Mig-6* code UTR also amplifies the untranslated region. The *Mig-6* code UTR therefore is a larger size as it incorporates both the translated and untranslated regions.

PCR product was run on a 1% agarose gel and photographed as follows:

1	2	3
---	---	---

1.	<i>Mig-6</i> code UTR
2.	<i>Mig-6</i> code
3.	DNA ladder

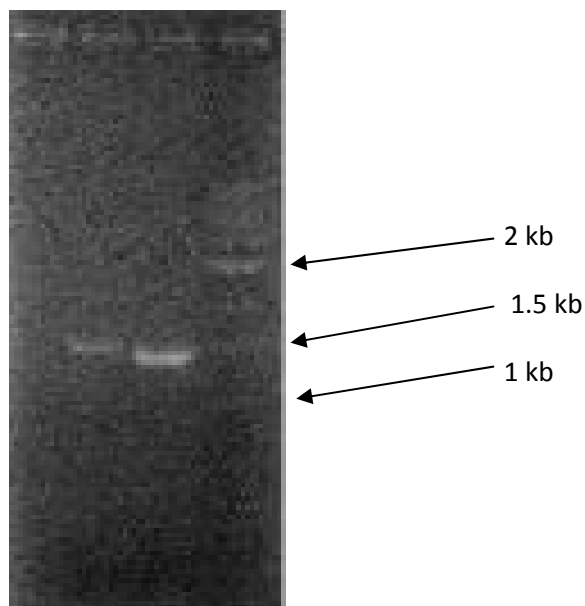


Fig 3.11 Shows the result of the Mig-6 PCR. Lanes 1 & 2 shows the band produced using the Mig-6 specific primers designed in house at ~1.5Kb and lane 3 shows the DNA ladder loaded on the gel.

3.8.1 ECOR I digestion of plasmids

Prior to sending our clones for sequencing we carried out a digestion using ECORI to prove that the clones we were sending contained the correct insert. We firstly carried out our cloning reaction using a **TOPO TA Cloning® Kit with pCR®2.1-TOPO®** as our vector. Sequencing results showed no mutations in the Mig-6 sequence of our H441 cells.

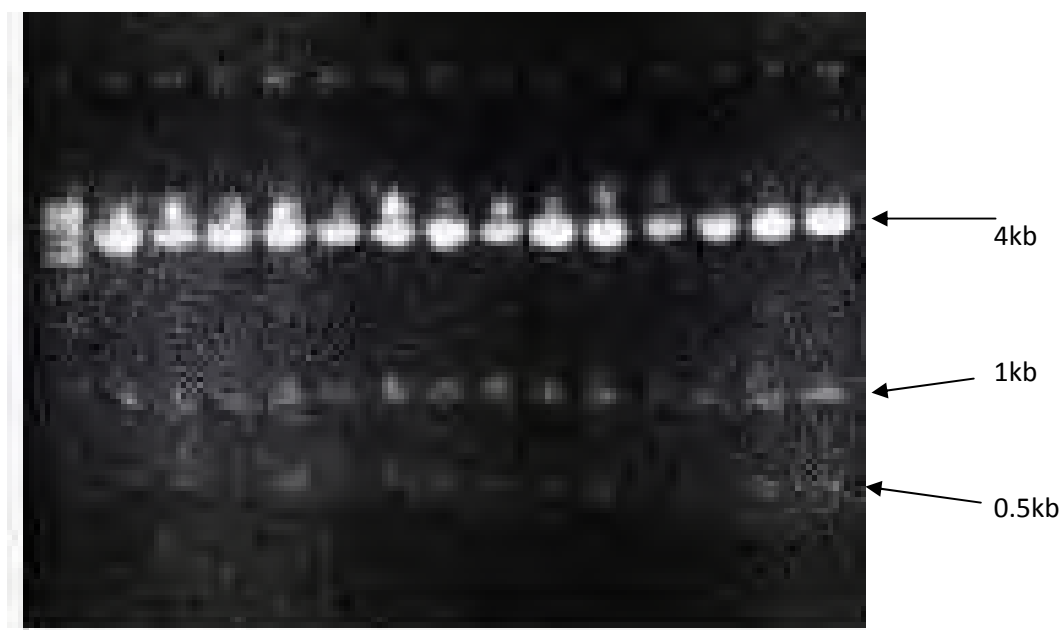


Fig 3.12 shows the results of ECOR I digestion of the plasmids. The bands at 4 kb are the vector whilst the bands at 1kb and 0.5kb are the Mig-6 sequence (the sequence itself contains an ECOR I site so we get three bands when a digestion has been successful).

Lane 1: 1kb DNA ladder

Lanes 2-15: plasmids 1 to 14

3.9 Western blot analysis of siRNA treated and untreated cells

The aim of our procedures was to look at the proteins involved in the EGF signalling pathway and ascertain whether their levels were altered when we silenced Mig-6 using siRNA treatment. We were also interested in looking at the involvement of Mig-6 in the HGF signalling pathway. It is already known that Mig-6 has a negative effect on HGF/Met-induced cell migration. In addition to this it has previously demonstrated that Mig06 expression is induced by HGF stimulation (73).

3.9.1 HGF Induction of Mig-6 in H441 and NHBE cells

This experiment was designed to look at the effect of HGF on cells where Mig-6 had been knocked out using siRNA. 40ng/ml HGF (hepatocyte growth factor) was administered for varying amounts of time and proteins isolated for Western blot analysis. The hypothesis was that if Mig-6 is involved in HGF signalling pathways then levels of Mig-6 proteins should change once HGF has been administered to the cells. We used H441 cell line as our epithelial cell model but also used NHBE (normal human bronchial epithelial) cells in our experiments so we would have data from both an epithelial cell line and from primary epithelial cells.

HGF Induction of Mig-6 in H441 cells:

We were unable to obtain any data for actin as a control so the densitometry analysis in this case will be a crude look at the changes occurring in this experiment assuming that the amount of protein loaded into each well was equal. We used the 0 min time point as a baseline to compare our other values to. An initial two-fold increase was observed at the 15 min timepoint. At 30mins post HGF administration, Mig-6 dropped to about $\frac{1}{2}$ that of the initial baseline level. At 2hrs post administration, mig-6 levels were ~3times that of the initial level and further increased to 4 times baseline by the 4 hour mark.

The administration of 40ng/ml HGF appears to have a stimulatory effect on the production of Mig-6 in H441 cells. Without an Actin loading control, we cannot normalize for the variability in the amount of protein loaded into each lane. The experiment would need to be repeated using our optimised Western blot protocol ensuring an Actin or other protein control is included to more accurately assess how Mig-6 levels are affected upon HGF administration.

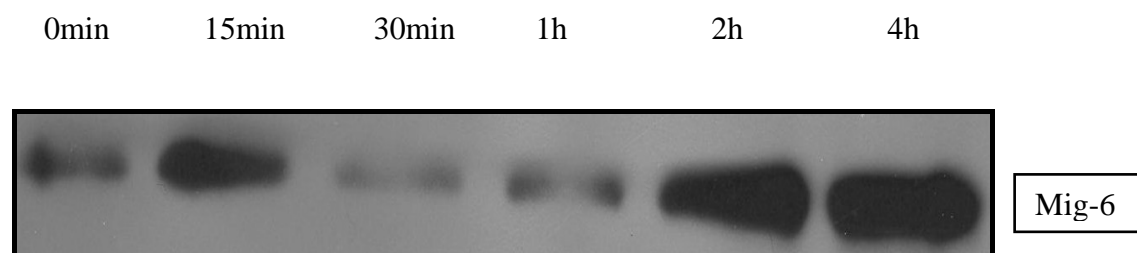


Fig 3.13a Shows the changes in Mig-6 levels in H441 epithelial cells observed at different time points post administration of 40ng/ml HGF (hepatocyte growth factor)

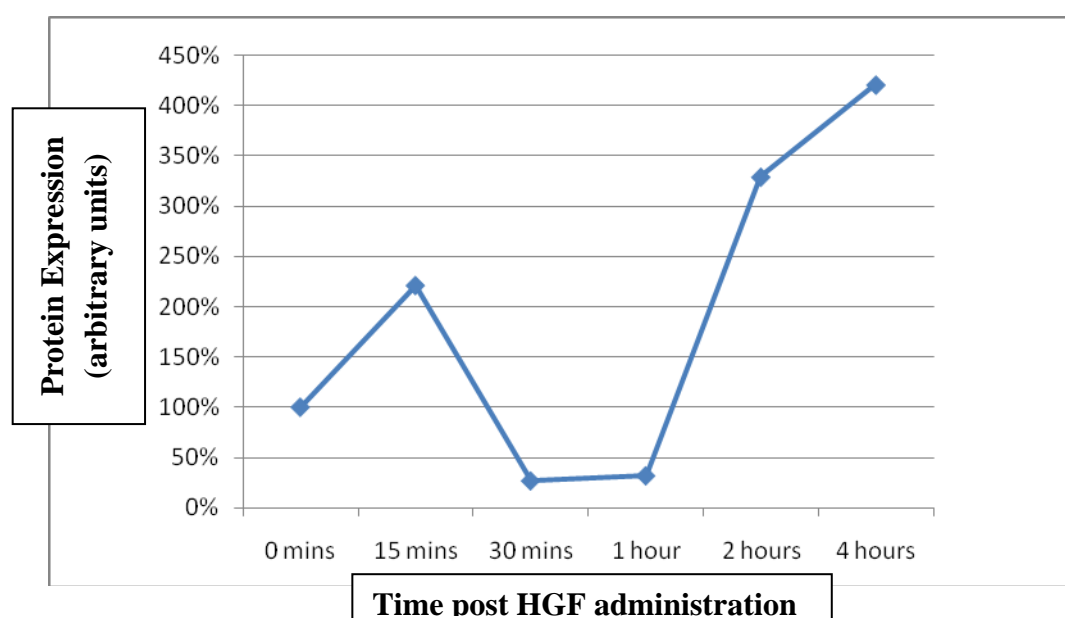


Figure 3.13b Densitometry analysis of western blot (fig 3.13a)

HGF Induction of Mig-6 in NHBE cells

Analysis of the Western blot by densitometry was carried out in order to look at what effects administration of HGF would have on different protein levels in NHBE cells. We normalized Mig-6 and EGFR expression using Actin as our control for equal protein loading.

Analysis showed little change in EGFR expression following treatment with HGF (as expected since HGF does not bind to EGFR) whereas changes in Mig-6 levels were clearly evident. Mig-6 expression quickly increased in expression and seemed to plateau after about

30 minutes to 1 hour. Mig-6 expression increased dramatically (~3 fold) between 15 minutes and 30 minutes post HGF administration. This dropped slightly to 2 ½ times the initial level at 1 hour before rising to almost four times the initial level at 2 hrs and dropping back to 2 ½ fold again at the four hour time-point.

This experiment would need to be repeated to see if this pattern would be repeated or not. It would also be interesting to look at other elements of the HGF pathway to see what effects administration of HGF would have on these and whether any of these elements is having any influence on the Mig-6 pattern observed in NHBE cells.

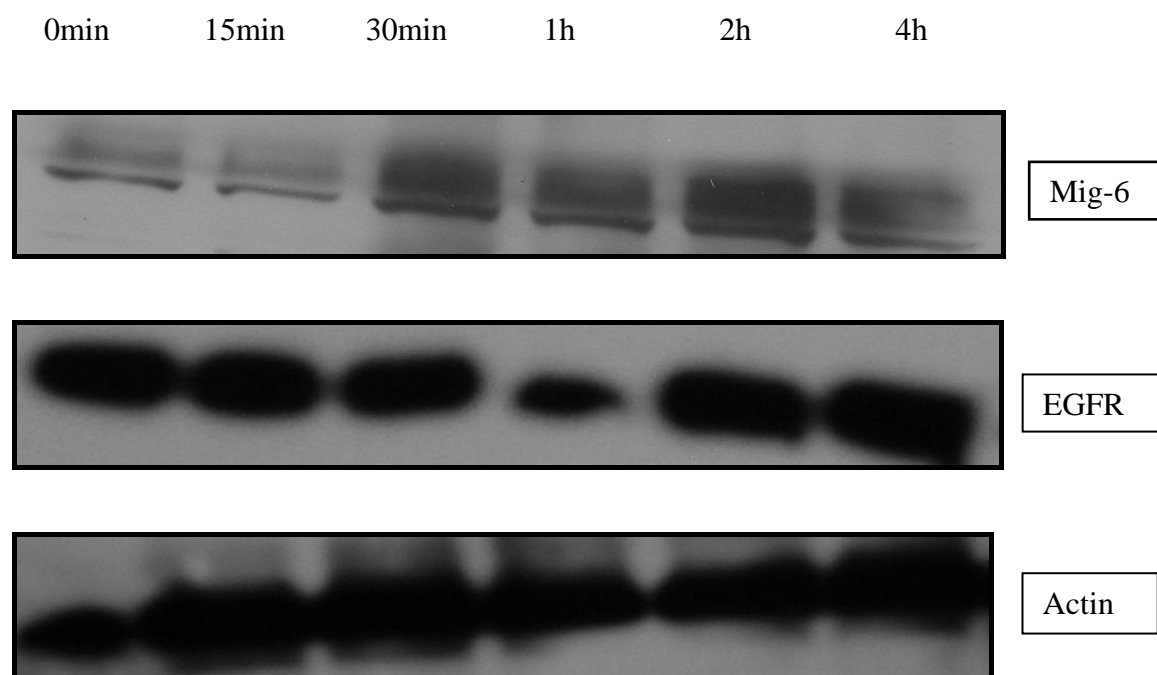


Fig 3.14a Shows the changes in Mig-6 and EGFR levels in normal human bronchial epithelial (NHBE) cells observed at different time points post administration of 40ng/ml HGF using actin as a loading control

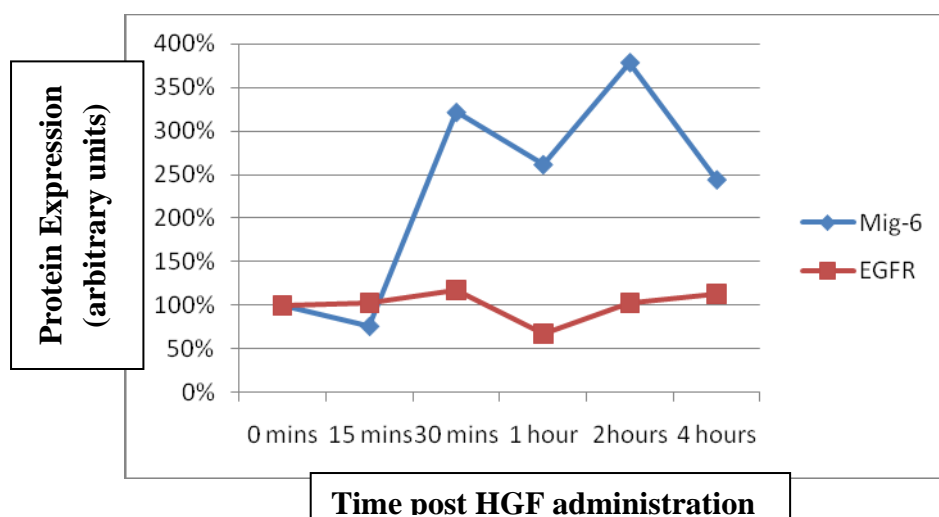


Figure 3.14b: densitometry analysis of fig. 3.14a

3.9.2 EGF Induction of Mig-6 in H441 and NHBE cells

As Mig-6 has been shown to be a negative regulator of EGFR we wanted to look at the effect of administering 40ng/ml of EGF to siRNA treated cells. Following this we also planned to look at the downstream elements of the EGF signalling pathway. First we established the effects of EGF on Mig-6 expression in cells.

EGF Induction of Mig-6 in H441 cells:

Unfortunately, since we do not have an Actin control we cannot normalize our Mig-6 expression levels to the exact amount of protein loaded in each lane. However, since we quantified the protein concentration in each sample and attempted to load equal amounts of protein into each lane we can establish that expression of Mig-6 appears to be sensitive to EGF.

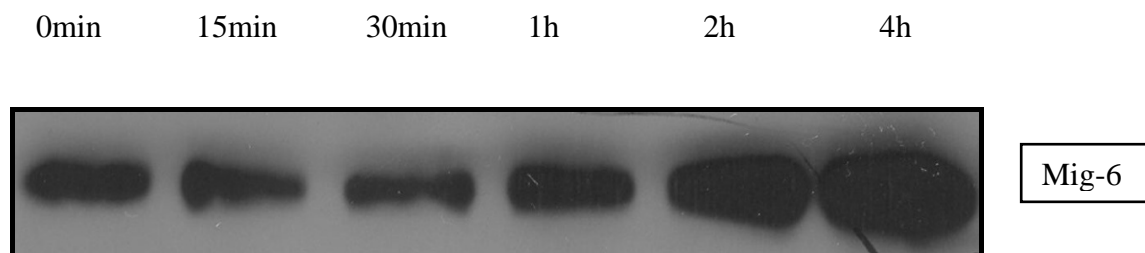


Fig 3.15a Shows the changes in Mig-6 levels in H441 cells observed at different time points post administration of 40ng/ml EGF (epidermal growth factor)

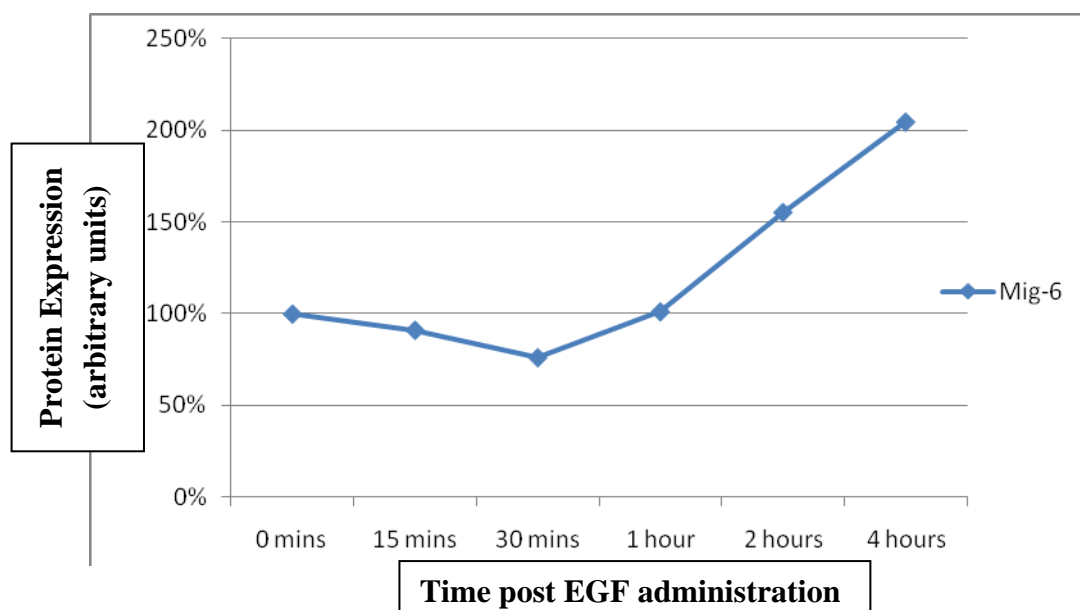


Figure 3.15b Analysis by densitometry showed that an initial decrease was observed post EGF administration but by the 1 hour mark, Mig-6 levels began to steadily increase. By the 4 hour time-point a two fold increase in Mig-6 is clearly evident.

EGF Induction of Mig-6 in NHBE cells

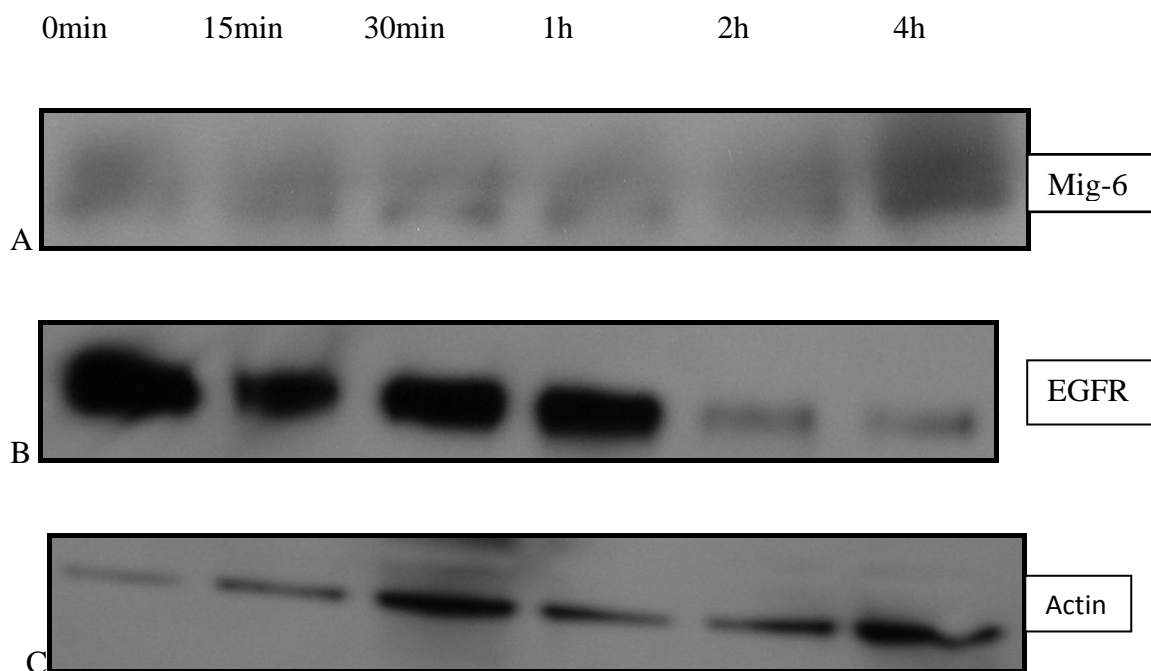


Fig 3.16a Shows the changes in Mig-6 and EGFR levels in normal human bronchial epithelial (NHBE) cells observed at different time points post administration of 40ng/ml EGF (epidermal growth factor). Blot B: Shows EGFR levels at several time points following the administration of 40ng/ml EGF. C shows the Actin control blot.

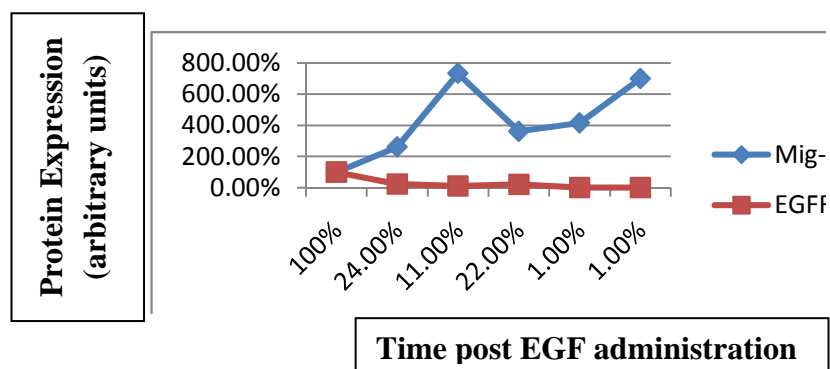


Figure 3.16b Analysis of the blots in fig 3.16a show that over the duration of the experiment, the levels of EGFR have remained relatively the same whilst the levels of Mig-6 have increased and decreased at different time points. The blots were normalised to Actin to allow for any loading differences.

Levels of Mig-6 began to rise from the 15 min point onwards with a large decrease occurring at 1 hour post EGF administration. This dip was then followed by a steady rise in levels at the remaining time points.

3.9.3 p-Akt levels in H441 cells in the presence and absence of EGF

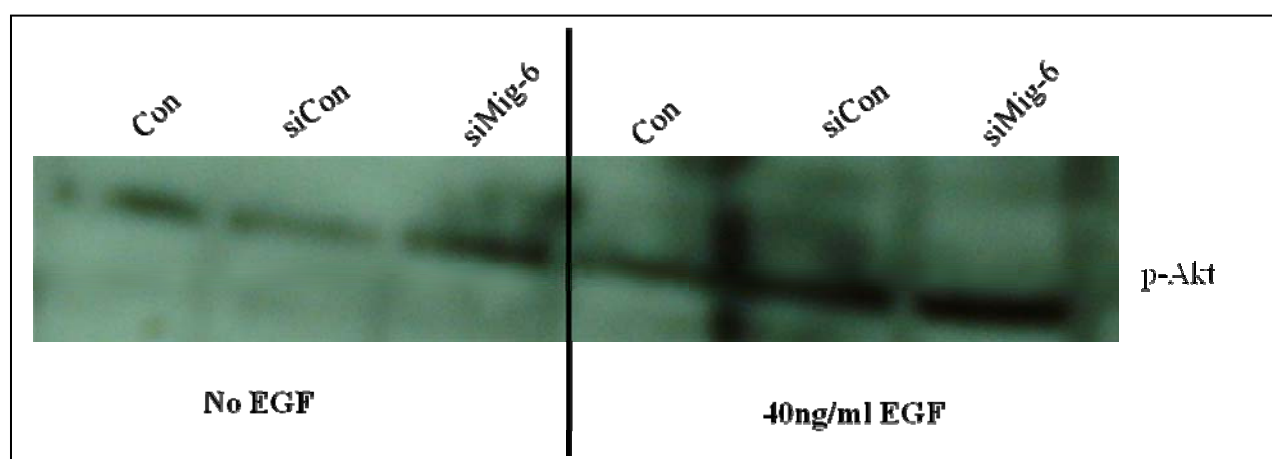


Fig 3.17a shows Western blot analysis for p-Akt in H441 cells treated with 50nm siRNA in the absence and in the presence of EGF

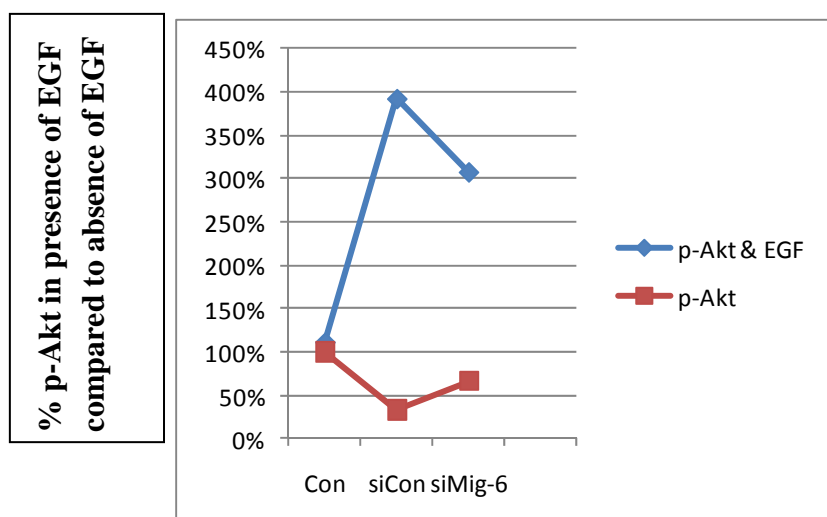


Figure 3.17b Analysis by densitometry showed that in the presence of 40ng/ml EGF, there was an increase in p-Akt levels in all our siRNA treated cells.

This experiment was designed to look at some of the elements of the EGFR signalling pathway in epithelial cells where Mig-6 has been knocked down. Half of the cells were subjected to siRNA treatment alone while the other half were treated in the presence of EGF. In the cells where not EGF was added it appears that there is an increase in p-Akt levels where Mig-6 has been knocked down using siRNA compared to the control where Mig-6 is expressed. In the cells where EGF has been administered, there appears to be no real difference between the levels of p-Akt in the control and siRNA treated cells.

The above blot (figure 3.17a) shows that in the cells treated with 40ng/ml EGF there appears to be increased p-Akt levels compared with the cells not treated with EGF.

The Western blot section of our experiments did not yield much data as we spent much of our time attempting to optimise our protocols to obtain useable data. We tried a number of things in order to optimise our protocol including:

1. Switching our washing buffer from PBST to TBST.
2. Changing our blocking buffer from 1% milk in PBST to 5% milk in TBST, also we switched from blocking at room temperature for one hour to a brief rinse in the new blocking buffer.
3. Altering the concentrations of both our primary and secondary antibodies and diluted them in 5% milk in TBST instead of 1% PBST.
4. We reduced the length of our washing steps from ten minutes to eight minutes.

These changes yielded better blots and would allow our lab to be able to repeat our experiments and yield useful data on the proteins involved in the signalling pathways of interest. The optimisation of the Western blot protocol was successful at the end of my

time in the lab but shown below (fig3.18) is an example of the result obtained using the new western blot protocol.

In the experiment below we treated the H441 cells with siRNA for 72hrs as detailed in section 2.1. After siRNA treatment we harvested RNA for real time PCR analysis and protein for Western blot analysis. As figure 3.18 below shows we successfully knocked down Mig-6 expression. This is illustrated again by the Western blot images above confirming the reduced expression of Mig6 in siRNA treated cells only.

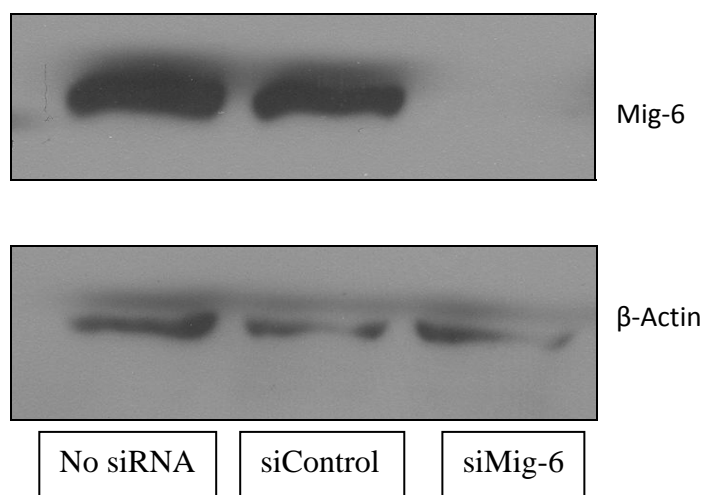


Fig 3.18a Western blot showing silencing of Mig-6 in H441 epithelial cells using 50nm siRNA

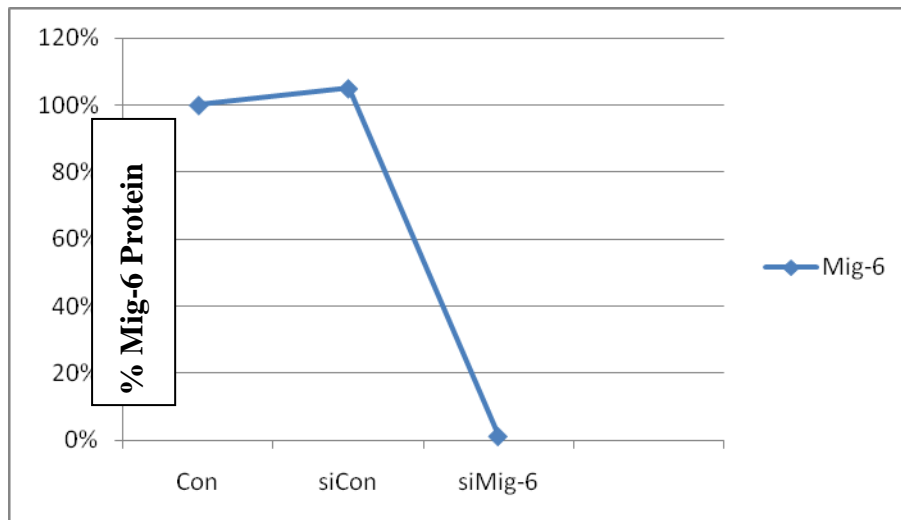


Figure 3.18b densitometry analysis of figure 3.18a indicated that there was a 99% decrease in Mig-6 levels when cells were treated with 50nm Mig-6 siRNA.

4. Discussion

Our lab was interested in studying the role of Mig-6 in the normal situation and in pathological conditions. By understanding the normal role that this gene plays we can gain greater insight to the processes that lead to disease when this gene is either deficient or completely absent. We proposed to carry out a number of different experiments in order to achieve our aims. Our studies were divided into animal studies and in vitro cell based studies.

Studies have previously been carried out to look at how Mig-6 is involved in the normal development of the lung and what happens when it is absent. We chose to look at the role of Mig-6 in an adult population of mice. An inducible knock out model was created for this purpose by crossing *Rosa26-Cre-ER^{T2}* (74) mice with *Mig-6^{flox/flox}* mice resulting in either *Rosa26-Cre-ERT2; Mig-6^{flox/flox}* (*Mig-6^{d/d}*) or *Mig-6^{flox/flox}* (*Mig-6^{f/f}*) mice. Upon administration of Tamoxifen to *Mig-6^{d/d}* mice Mig-6 was knocked down. This provided us with adult mice lacking the Mig-6 gene and afforded us the opportunity to look at any effects that this would have on these mice, using the *Mig-6^{f/f}* mice as a control.

Our *in vitro* studies looked at an epithelial cell line and an endothelial cell line. Using siRNA, Mig-6 expression was successfully silenced in both cell types. In these cells we looked at cell viability following Mig-6 silencing. We also intended to look at elements of the EGF signalling pathway and how they are affected by silencing Mig-6 expression.

Our initial experiments focused on the inducible knock out model. Once the Tamoxifen treated mice had reached six months in age (4 months post Tamoxifen treatment) they were sacrificed and the lung tissue harvested. Some of the harvested tissue was processed to paraffin wax blocks and set aside for histological staining. The rest of the tissues were used

for molecular studies. mRNA was extracted and used for real time quantitative PCR analysis for Mig-6, CCSP, T1-alpha, SP-C and Muc5ac using 18s rRNA as a control.

Figure 3.1 shows the results of the real time quantitative PCR analysis of Mig-6^{+/+}, Mig-6^{-/-}, Mig-6^{f/f} and Mig-6^{d/d} mice for Mig-6 RNA. We expected that Tamoxifen treatment would cause the ablation of Mig-6 in adult Mig-6^{d/d} mice. *Rosa26-Cre-ERT2* mice were crossed with Mig-6^{fllox/fllox} (Mig-6^{f/f}) mice resulting in our Mig-6^{d/d} mice. As expected, administration of Tamoxifen to both of these populations of mice resulted in the successful ablation of Mig-6 in the Mig-6^{d/d} mice while Mig-6 expression was similar to normal adult levels in the Mig-6^{f/f} control mice. In this important experiment to test our conditional knockout model, we demonstrated that expression of Mig-6 was comparable between wild type mice and Mig-6^{f/f} mice and between Mig-6^{-/-} mice and Mig-6^{d/d} mice. Therefore, this allowed us to use our inducible knockout model to study the effects that the loss of Mig-6 would have (if any) in adult mice.

Comparison of the morphology of f/f and d/d adult mouse lungs

It has been shown previously in our lab that Mig-6^{-/-} mice exhibit altered lung morphology (increased alveolar spaces and altered septation compared with wild type mice (5). However, Mig-6 expression is ablated from conception in Mig-6^{-/-} mice which hinders our efforts to elucidate the role of Mig-6 in adult mice. Therefore, we chose to carry out a set of experiments to compare lung morphology in Tamoxifen treated Mig-6^{f/f} and Mig-6^{d/d} mice. Lung sections from our Tamoxifen treated mice were stained using Haematoxylin and Eosin to show general morphology. Both the Mig-6^{d/d} and Mig-6^{f/f} mice showed normal lung morphology and no differences were noted between the two genotypes. Measurement of the alveolar spaces of Mig-6^{+/+}, Mig-6^{-/-}, Mig-6^{f/f} and Mig-6^{d/d} mice showed that while the Mig-6^{-/-} had significantly larger alveolar spaces, specific depletion of Mig-6 in adult mice (Mig-6^{d/d})

using Tamoxifen did not lead to any significant differences in alveolar size when compared to wild type mice and Mig-6^{f/f} mice.

Results of the histological analysis shows that when Mig-6 is ablated in adult mice using Tamoxifen, the lung tissue remains morphologically similar to the wild type untreated mice. These mice were at the adult stage of life and therefore their lungs were fully formed before treatment to induce ablation of Mig-6 commenced. Our results appear to indicate that once lung development is complete, Mig-6 may not have any noticeable effect on lung morphology.

Pulmonary markers-CCSP, SP-C, T1 alpha, Muc5ac

There is a significant difference in T1 alpha levels between Mig-6^{+/+} and Mig-6^{-/-} mice with Mig-6^{-/-} having greatly reduced expression of T1 alpha in the lung (see Figure 3.5). No significant difference in T1 alpha expression in the lung was measured between f/f and d/d mice, nor did T1 alpha levels in these mice differ significantly from the wild type levels measured. This is an interesting result to note as T1 alpha levels were not affected when Mig-6 is knocked out at the adult stage of life while if it is knocked out in the germline then the resulting Mig-6^{-/-} mice have significantly reduced T1 alpha levels, this may point to a decrease in type I airway epithelial cells as T1 alpha is used as a marker for this cell type. Our data indicate that Mig-6 and T1 alpha expression are both linked within the developmental process and that defective lung development in Mig-6^{-/-} mice may contribute to the decreased expression of this important alveolar type I epithelial cell.

SP-C levels in Mig-6^{f/f} and Mig-6^{d/d} mice are unchanged from those seen in wild type levels while levels in Mig-6^{-/-} mice are greatly elevated. Because the only difference in SP-C levels was seen in mice where Mig-6 is knocked out prior to foetal development this may point to a link between Mig-6 and SP-C in the developmental stages of life. It may be that Mig-6 has a

regulatory role and prevents overexpression of SP-C during development and when this control is removed SP-C levels increase greatly. It is interesting to note that SP-C expression has been found to increase when mechanical strain in the lung is increased (65) SP-C can be used as a marker for type II epithelial cells so it may be that in mechanical strain on the lung, type II airway epithelial cell expression is increased. Lung morphology has developed normally in the Tamoxifen treated Mig-6^{d/d} mice and no increase in SP-C was observed, suggesting that Mig-6 expression does not directly control SP-C levels. However, SP-C is greatly elevated in the lungs of Mig-6^{-/-} mice suggesting that the increased SP-C expression observed here may be due to increased mechanical strain as a consequence of developmental defects in the lung morphology of Mig-6^{-/-} mice. Further investigations would be needed to confirm or disprove this hypothesis.

MUC5AC levels in Mig-6^{f/f} and Mig-6^{d/d} mice are not significantly different to that of wild type mice. The Mig-6^{-/-} mice on the other hand had a dramatic increase in MUC5AC. This would suggest that MUC5AC levels may be linked with Mig-6 at a developmental stage but not once the lungs have been formed as in our Mig-6^{f/f} and Mig-6^{d/d} mice. As previously mentioned, MUC5AC levels have been seen to be increased in airway disease (75) while decreased Mig-6 levels are often seen in airway disease. This might suggest that there could be a regulatory link between Mig-6 and MUC5AC.

In the case of the CCSP measurements, it appears as though the Mig-6^{d/d} group express about half the levels of CCSP compared with the wild type and Mig-6^{f/f} mice. However, there was a large degree of variability noted in these measurements so despite obtaining significant differences, we would need to repeat this experiment to increase our confidence in our data for this marker. However, one must also consider the possibility that Mig-6 expression plays a role in regulating some functions of Clara cells in adult mice. If CCSP expression is

consistently decreased in Mig-6^{d/d} mice, then further experimentation should be carried out to determine the role of Mig-6 in promoting CCSP expression.

Measurement of the molecular markers in our different mouse genotypes provided some interesting results. In all four cases there was a significant difference noted between wild type and Mig-6 knockout mice. In all but the CCSP measurements, no significant difference was noted between our two genotypes of Tamoxifen treated mice. These levels were also comparable to the wild type measurements obtained at the same time. These data seem to indicate that Mig-6 does not directly regulate the expression of SP-C, T1 alpha and MUC5AC in adult mouse lung cells.

In repeating the experiment we would also increase the number of animals of each genotype tested account for this variability and this would allow us to be more confident that our results would accurately represent the genotypes in question.

In vitro cell studies

The next set of experiments was designed to allow us to look at the effect of Mig-6 in specific cell types *in vitro* and gain a greater insight into the signalling pathways that are influenced when Mig-6 is knocked out. We looked at an epithelial cell line and an endothelial cell line to ascertain whether any differences would be noted when we knocked out Mig-6 in these cell types or whether the same signalling pathways would be affected in both cell types.

The first step was to use RNA interference to knock out Mig-6 expression. This was successfully achieved using a concentration of 50nm siRNA. RNA was extracted from the treated cells and real time quantitative PCR analysis for Mig-6 showed that we were successful in silencing Mig-6 expression in both cell lines (See Figure 3.8 and 3.9). Following this we moved onto the next set of *in vitro* experiments. We carried out a cell

viability assay to look at whether silencing Mig-6 expression would have any effect on the viability of the cells. Interestingly, our results showed that the number of viable epithelial cells increased following silencing of Mig-6 expression using siRNA while cell viability was seen to decrease when Mig-6 expression was silenced in endothelial cells.

We hypothesised from these results that in an epithelial cell population, silencing Mig-6 expression may cause an increase in cellular proliferation which would explain the increase in viable cells measured. Another potential reason for the increased viable cells could be that in the absence of Mig-6, regular cell death does not occur at the same rate as normal resulting in increased cellular survival.

A decrease in viable cells was observed when Mig-6 expression was silenced in endothelial cells. This led us to hypothesise that there was increased apoptosis in this cell population or that there was a decreased rate of cellular proliferation. To investigate this further we could use immunohistochemical staining for cleaved caspase 3 to look at apoptosis.

This may be linked to the pathways affected when Mig-6 is removed and our next step was to investigate these pathways by looking at various protein levels in cells where Mig-6 has been silenced as well as cells where Mig-6 levels remain as normal. Because Mig-6 is known to be involved in the EGF signalling pathway that was our initial focus to see how downstream elements would be affected upon silencing of Mig-6 expression. Activation of the EGF receptor results in activation of various downstream signalling cascades including the RAS/ERK pathway, the PI3K/Akt pathway and the JAK/STAT pathway which coordinate to promote cellular survival and proliferation (76).

Mig-6 has been shown to be a negative regulator of EGFR signalling (30) so when it is no longer present then EGF receptor activation kinetics are prolonged and the above mentioned pathways (Ras/Erk; PI-3K/Akt; and JAK/STAT) may be activated for longer than normal

leading to changes in cellular survival. It was interesting to note that when Mig-6 was silenced it had differing effects on the survival of epithelial cells and endothelial cells. To understand potential reasons for this it was necessary to look at levels of the individual components of each signalling pathway involved to see at which point in the signalling the differences occurred.

HGF signalling has also been linked to Mig-6 which led us to decide to look at what effect HGF signalling pathways would have on Mig-6 expression and related signalling pathways. We intended to look at both EGF-dependent and HGF-dependent induction of Mig-6 expression in lung epithelial cells treated with siRNA alongside untreated cells. In particular, we were interested in whether administration of either EGF or HGF would significantly affect the levels of Mig-6 expression and if so how long it would take to occur. We used H441 cells again as our epithelial cell line but this time we also used NHBE cells as a primary epithelial cell line to gain data from both a cell line and primary human cells. In addition to investigating expression of Mig-6, we also intended to look at levels of various proteins following EGF/HGF administration using Western blot analysis. The protein levels we were interested include: total Akt and activated phospho-Akt (p-Akt), total mTor and activated p-mTor, total EGFR expression and activated p-EGFR.

Initially we experienced difficulty in getting our Western blot protocol to work sufficiently and as a result spent a large amount of our time altering the protocol in an attempt to optimise it. The changes (altering buffers, blocking solution, changing antibody concentration and altering incubation times) yielded better blots and would allow our lab to be able to repeat our experiments and yield useful data on the proteins involved in the signalling pathways of interest. The optimisation of the Western blot protocol was successful at the end of my time in the time in the lab. Had there been more time we would have carried out our planned investigation of the proteins involved in the pathways I mentioned earlier. In addition to

looking at the changes seen at the protein level, it would also be interesting to look at any changes seen at the RNA level to obtain the full picture. From the limited data we obtained it appears that administration of EGF to Mig-6 siRNA treated cells can cause an increase in the Mig-6 protein levels between 1 and 4 hours post-administration of EGF. This experiment would need to be repeated to ascertain whether this is truly the case.

Our results showed some interesting data which provides further routed of investigation of the role of Mig-6. Of particular interest were the results of the *in vitro* studies which showed differing effects on cell survival/proliferation when comparing lung epithelial and endothelial cells. The next step would be to use our improved Western blot protocol to obtain more data on the different proteins affected in both cell types following silencing of Mig-6. This would lead to a greater understanding of how these cells are affected in vitro and perhaps lead to further research into potential therapies to overcome the effects of a loss of Mig-6.

Future directions for this research:

As Mig-6 is a stress induced gene our lab is interested in looking at what happens when Mig-6 is knocked out at the adult stage of life but this time exposing the animals to a stress (such as cigarette smoke for example) and examining whether this would show different effects than when we simply just knocked out Mig-6 in adult mice. In our experiments the lungs of induced knockout mice appeared to remain normal so it would be of interest to investigate whether the same would be true when the induced knockout mice were also exposed to stress.

Because of the differences noted between effects on siRNA treated epithelial and endothelial cells, our lab is interested in pursuing this and looking in more detail at the role of Mig-6 in both types of cells.

This inducible knockout model would also be beneficial in studying the role of Mig-6 expression in cancer, especially in light of its putative role as a tumour suppressor (2).

By understanding the role that Mig-6 plays in the normal individual, we can gain a better insight into what happens when Mig-6 is absent and where things go wrong at a molecular level. This will enable the development of more treatment options and ways to overcome the effects which result from the absence of Mig-6.

References

1. Makkinje, A., Quinn, D., Chen, A., Cadilla, C., Force, T., Bonventre, J. & Kyriakis, J. 2000. Gene 33/Mig-6, a transcriptionally inducible adapter protein that binds GTP-Cdc42 and activates SAPK/JNK. A potential marker transcript for chronic pathologic conditions, such as diabetic nephropathy. Possible role in the response to persistent stress. *J Biol Chem*, 275, 17838-47.
2. Ferby, I., Reschke, M., Kudlacek, O., Knyazev, P., Pant, G., Amann, K., Sommergruber, W., Kraut, N., Ullrich, A., Fessler, R. & Klein, R. 2006. Mig6 is a negative regulator of EGF receptor-mediated skin morphogenesis and tumor formation. *Nat Med*, 12, 568-73.
3. Zhang, Y., Staal, B., Su, Y., Swaitek, P., Zhao, P., Cao, B., Resau, J., Sigler, R., Bronson, R. & Vande Woude, G. 2007. Evidence that MIG-6 is a tumor-suppressor gene. *Oncogene*, 26, 269-76.
4. Zhang, Y. & Vande Woude, G. 2007. Mig-6, signal transduction, stress response and cancer. *Cell Cycle*, 6, 507-13.
5. Jin, N., Cho, S., Raso, M., Wistuba, I., Smith, Y., Yang, Y., Kurie, J., Yen, R., Evans, C., Ludwig, T., Jeong, J. & DeMayo, F. 2009. Mig-6 is required for appropriate lung development and to ensure normal adult lung homeostasis. *Development*, 136, 3347-56.
6. Jin, N., Gilbert, J., Broaddus, R., DeMayo, F. & Jeong, J. 2007. Generation of a Mig-6 conditional null allele. *Genesis*, 45, 716-21.
7. Wert, S.E. et al. (1993) Transcriptional elements from the human SP-C gene direct expression in the primordial respiratory epithelium of transgenic mice. *Dev. Biol.* 156, 426–443

8. Ray, M.K. et al. (1996) Immunohistochemical localization of mouse Clara cell 10-KD protein using antibodies raised against the recombinant protein. *J. Histochem. Cytochem.* 44, 919–927
9. Peters, K. et al. (1994) Targeted expression of a dominant negative FGF receptor blocks branching morphogenesis and epithelial differentiation of the mouse lung. *EMBO J.* 13, 3296–3301
10. Simonet, W.S. et al. (1995) Pulmonary malformation in transgenic mice expressing human keratinocyte growth factor in the lung. *Proc. Natl. Acad. Sci. USA* 92, 12461–12465
11. DeMayo, F.J. and Tsai, S.Y. (2001) Targeted gene regulation and gene ablation. *Trends Endocrinol. Metab.* 12, 348–353
12. <http://www.cdc.gov/niosh/docs/2004-154c/pdfs/2004-154c-ch1.pdf>
13. Matthay, M., Folkesson, H. & Clerici, C. 2002. Lung epithelial fluid transport and the resolution of pulmonary edema. *Physiol Rev*, 82, 569-600.
14. Hermans, C. & Bernard, A. 1999. Lung epithelium-specific proteins: characteristics and potential applications as markers. *Am J Respir Crit Care Med*, 159, 646-78.
15. <http://www.childrens-mercy.org/pa/images/respirat.gif>
16. Hislop, A. 2002. Airway and blood vessel interaction during lung development. *J Anat*, 201, 325-34.
17. Desai, T. & Cardoso, W. 2002. Growth factors in lung development and disease: friends or foe? *Respir Res*, 3, 2.
18. American lung association: lung disease data 2008
<http://www.lungusa.org/atf/cf/{7A8D42C2-FCCA-4604-8ADE-7F5D5E762256}/LDD08.PDF>

19. American lung association
20. Ireland needs healthier airways and lungs- the evidence. INHALE Report, 2nd Edition. A Compilation of Statistical Data by Dr Neil Brennan, Suzanne McCormack and Dr Terry O'Connor. The Irish Medical Journal Feb 2008 (supplement)
21. Guidelines for Clinical Management of Lung Cancer February 2004
http://www.imj.ie/Archive/Lung_Cancer_Guidelines.pdf
22. <http://www.merck.com/mmpe/sec05/ch062/ch062b.html#sec05-ch062-ch062b-1405>
23. Li Mao, Ralph H. Hruban, Jay O. Boyle, Melvyn Tockman, and David Sidransky. Detection of Oncogene Mutations in Sputum Precedes Diagnosis of Lung Cancer Cancer Research 54, 1634-1637. April 1994
24. Collins, LG., Haines, C, Perkel, R.,and Enck, R.E. Lung Cancer: Diagnosis and Management. *Am Fam Physician*. 2007 Jan 1;75(1):56-63.
25. Normanno N, De Luca A, Bianco C, Strizzi L, Mancino M, Maiello MR, Carotenuto A, De Feo G, Caponigro F, Salomon DS). Epidermal growth factor receptor (EGFR) signaling in cancer. (Gene. 2006 Jan 17;366(1):2-16. Epub 2005 Dec 27.
26. Feil, R., Brocard, J., Mascrez, B., Lemeur, M., Metzger, D. & Chambon, P. 1996. Ligand-activated site-specific recombination in mice. *Proc Natl Acad Sci U S A*, 93, 10887-90.
27. Branda, C. & Dymecki, S. 2004. Talking about a revolution: The impact of site-specific recombinases on genetic analyses in mice. *Dev Cell*, 6, 7-28
28. Sangiorgi, E., Shuhua, Z. & Capecchi, M. 2008. In vivo evaluation of PhiC31 recombinase activity using a self-excision cassette. *Nucleic Acids Res*, 36, e134.
29. <http://jaxmice.jax.org/research/cre/introduction.html>

Introduction to Cre-lox technology, the Jackson Laboratory

30. http://deposit.ddb.de/cgi-bin/dokserv?idn=97557230x&dok_var=d1&dok_ext=pdf&filename=97557230x.pdf
31. Hameyer, D., Loonstra, A., Eshkind, L., Schmitt, S., Antunes, C., Groen, A., Bindels, E., Jonkers, J., Krimpenfort, P., Meuwissen, R., Rijswijk, L., Bex, A., Berns, A. & Bockamp, E. 2007. Toxicity of ligand-dependent Cre recombinases and generation of a conditional Cre deleter mouse allowing mosaic recombination in peripheral tissues. *Physiol Genomics*, 31, 32-41.
32. Dhanasekaran, N. 1998. Cell signaling: an overview. *Oncogene*, 17, 1329-30.
33. http://alisoniguel.com/staffpages/tlhenson/Teacher/APBio/Lecture_Notes_APbio_04-05/Ch11_Lecture_Notes.pdf
34. Hubbard, S. & Miller, W. 2007. Receptor tyrosine kinases: mechanisms of activation and signaling. *Curr Opin Cell Biol*, 19, 117-23.
35. Cadena, D. & Gill, G. 1992. Receptor tyrosine kinases. *FASEB J*, 6, 2332-7.
36. Gotoh, N. 2009. Feedback inhibitors of the epidermal growth factor receptor signaling pathways. *Int J Biochem Cell Biol*, 41, 511-5.
37. Bose, R. & Zhang, X. 2009. The ErbB kinase domain: structural perspectives into kinase activation and inhibition. *Exp Cell Res*, 315, 649-58.
38. Oda, K., Matsuoka, Y., Funahashi, A. & Kitano, H. 2005. A comprehensive pathway map of epidermal growth factor receptor signaling. *Mol Syst Biol*, 1, 2005.0010.
39. Yarden, Y. 2001. The EGFR family and its ligands in human cancer. signalling mechanisms and therapeutic opportunities. *Eur J Cancer*, 37 Suppl 4, S3-8.
40. Zhang, X., Gureasko, J., Shen, K., Cole, P. & Kuriyan, J. 2006. An allosteric mechanism for activation of the kinase domain of epidermal growth factor receptor. *Cell*, 125, 1137-49.

41. Kheradmand, F., Rishi, K. & Werb, Z. 2002. Signaling through the EGF receptor controls lung morphogenesis in part by regulating MT1-MMP-mediated activation of gelatinase A/MMP2. *J Cell Sci*, 115, 839-48.
42. Moghal, N. & Sternberg, P. 1999. Multiple positive and negative regulators of signaling by the EGF-receptor. *Curr Opin Cell Biol*, 11, 190-6.
43. Reschke, M., Ferby, I., Stepniak, E., Seitzer, N., Horst, D., Wagner, E. & Ullrich, A. 2010. Mitogen-inducible gene-6 is a negative regulator of epidermal growth factor receptor signaling in hepatocytes and human hepatocellular carcinoma. *Hepatology*, 51, 1383-90.
44. Zhang, X., Pickin, K., Bose, R., Jura, N., Cole, P. & Kuriyan, J. 2007a. Inhibition of the EGF receptor by binding of MIG6 to an activating kinase domain interface. *Nature*, 450, 741-4.
45. Anastasi, S., Baietti, M., Frosi, Y., Aalem, S. & Segatto, O. 2007. The evolutionarily conserved EBR module of RALT/MIG6 mediates suppression of the EGFR catalytic activity. *Oncogene*, 26, 7833-46.
46. Iejima, D., Minegishi, Y., Takenaka, K., Siswanto, A., Watanabe, M., Huang, L., Watanabe, T., Tanaka, F., Kuroda, M. & Gotoh, N. 2010. FRS2beta, a potential prognostic gene for non-small cell lung cancer, encodes a feedback inhibitor of EGF receptor family members by ERK binding. *Oncogene*.
47. Nicholson, S., Metcalf, D., Sprigg, N., Columbus, R., Walker, F., Silva, A., Cary, D., Willson, T., Zhang, J., Hilton, D., Alexander, W. & Nicola, N. 2005. Suppressor of cytokine signaling (SOCS)-5 is a potential negative regulator of epidermal growth factor signaling. *Proc Natl Acad Sci U S A*, 102, 2328-33.

48. Laederich, M., Funes-Duran, M., Yen, L., Ingalla, E., Wu, X., Carraway, K. R. & Swenney, C. 2004. The leucine-rich repeat protein LRIG1 is a negative regulator of ErbB family receptor tyrosine kinases. *J Biol Chem*, 279, 47050-6.
49. H. Ohmichi, U. Koshimizu, K. Matsumoto and T. Nakamura. 1998. Hepatocyte growth factor (HGF) acts as a mesenchyme-derived morphogenic factor during fetal lung development *Development* 125, 1315-1324
50. Ricci, G., Catizone, A. & Galdieri, M. 2006. Expression and functional role of hepatocyte growth factor and its receptor (c-met) during fetal mouse testis development. *J Endocrinol*, 191, 559-70.
51. Sakkab, D., Lewitzky, M., Posern, G., Schaeper, U., Sachs, M., Birchmeier, W. & Feller, S. 2000. Signaling of hepatocyte growth factor/scatter factor (HGF) to the small GTPase Rap1 via the large docking protein Gab1 and the adapter protein CRKL. *J Biol Chem*, 275, 10772-8.
52. Zachow, R. & Uzumcu, M. 2007. The hepatocyte growth factor system as a regulator of female and male gonadal function. *J Endocrinol*, 195, 359-71.
53. Peruzzi, B. & Bottaro, D. 2006. Targeting the c-Met signaling pathway in cancer. *Clin Cancer Res*, 12, 3657-60.
54. Ma, P., Tretiakova, M., Nallasura, V., Jagadeeswaran, R., Husain, A. & Salgia, R. 2007. Downstream signalling and specific inhibition of c-MET/HGF pathway in small cell lung cancer: implications for tumour invasion. *Br J Cancer*, 97, 368-77.
55. Mizuno, S., Matsumoto, K., Li, M. & Nakamura, T., Ma, P., Tretiakova, M., Nallasura, V., Jagadeeswaran, R., Husain, A. & Salgia, R. 2007. Downstream signalling and specific inhibition of c-MET/HGF pathway in small cell lung cancer: implications for tumour invasion. *Br J Cancer*, 97, 368-77.

56. Huntsman, D., Resau, J., Klineberg, E. & Auersperg, N. 1999. Comparison of c-met expression in ovarian epithelial tumors and normal epithelia of the female reproductive tract by quantitative laser scan microscopy. *Am J Pathol*, 155, 343-8.
57. Korobko, I., Zinov'eva, M., Aallakhverdiev, A., Zborovskaia, I. & Svwordlov, E. 2007. [c-Met and HGF expression in non-small-cell lung carcinomas]. *Mol Gen Mikrobiol Virusol*, 18-21.
58. Hackel, P., Gishizky, M. & Ullrich, A. 2001. Mig-6 is a negative regulator of the epidermal growth factor receptor signal. *Biol Chem*, 382, 1649-62.
59. Bry, K., Whitsett, J. & Lappalainen, U. 2007. IL-1beta disrupts postnatal lung morphogenesis in the mouse. *Am J Respir Cell Mol Biol*, 36, 32-42
60. Copens, J., Van Winkle, L., Pinkerton, K. & Plopper, C. 2007. Distribution of Clara cell secretory protein expression in the tracheobronchial airways of rhesus monkeys. *Am J Physiol Lung Cell Mol Physiol*, 292, L1155-62.
61. Hackett, B. & Gitlin, J. 1992. Cell-specific expression of a Clara cell secretory protein-human growth hormone gene in the bronchiolar epithelium of transgenic mice. *Proc Natl Acad Sci U S A*, 89,9079-83.
62. Williams, M., Cao, Y., Hinds, A., Rishi, A. & Wetterwald, A. 1996. T1 alpha protein is developmentally regulated and expressed by alveolar type I cells, choroid plexus, and ciliary epithelia of adult rats. *Am J Respir Cell Mol Biol*, 14, 577-85.
63. Lyra, P. & Diniz, E. 2007. The importance of surfactant on the development of neonatal pulmonary diseases. *Clinics (Sao Paulo)*, 62, 181-90.
64. <http://www.leonenkoresearch.uwaterloo.ca/data/amyloidosis%20review.pdf>
65. Nakamura, T., Liu, M., Mourgeon, E., Slutsky, A. & Post, M. 2000. Mechanical strain and dexamethasone selectively increase surfactant protein C and tropoelastin gene expression. *Am J Physiol Lung Cell Mol Physiol*, 278, L974-80.

66. <http://www.genecards.org/cgi-bin/carddisp.pl?gene=Muc5ac>
67. Groneberg, D., Eynott, P., Oates, T., Lim, S., Wu, R., Carlstedt, I., Nicholson, A. & Chung, K. 2002. Expression of MUC5AC and MUC5B mucins in normal and cystic fibrosis lung. *Respir Med*, 96, 81-6.
68. Thompson, A., Robbins, R., Romberger, D., Sisson, J., Spurzem, J., Teschler, H. & Rennard, S. 1995. Immunological functions of the pulmonary epithelium. *Eur Respir J*, 8, 127-49.
69. Puchelle, E. & Peault, B. 2000. Human airway xenograft models of epithelial cell regeneration. *Respir Res*, 1, 125-8.
70. Anastasi, S., Fiorentino, L., Fiorini, M., Fraioli, R., Sala, G., Castellani, L., Alem, S., Alimandi, M. & Segatto, O. 2003. Feedback inhibition by RALT controls signal output by the ErbB network. *Oncogene*, 22, 4221-34.
71. Ballaro, C., Ceccarelli, S., Tiveron, C., Tatangelo, L., Salvatore, A., Segatto, O. & Alem, S. 2005. Targeted expression of RALT in mouse skin inhibits epidermal growth factor receptor signalling and generates a Waved-like phenotype. *EMBO Rep*, 6, 755-61.
72. http://www.mnstate.edu/provost/MTT_Proliferation_Protocol.pdf
73. Pante, G., Thompson, J., Lamballe, F., Iwata, T., Ferby, I., Barr, F., Davies, A., Maina, F. & Klein, R. 2005. Mitogen-inducible gene 6 is an endogenous inhibitor of HGF/Met-induced cell migration and neurite growth. *J Cell Biol*, 171, 337-48.
74. De Luca, C., Kowalski, T., Zhang, Y., Elmquist, J., Lee, C., Kilimann, M., Ludwig, T., Liu, S. & Chua, S. J. 2005. Complete rescue of obesity, diabetes, and infertility in db/db mice by neuron-specific LEPR-B transgenes. *J Clin Invest*, 115, 3484-93.
75. Kraft, M., Aadler, K., Ingram, J., Crews, A., Atkinson, T., Cairns, C., Krause, D. & Chu, H. 2008. Mycoplasma pneumoniae induces airway epithelial cell expression of MUC5AC in asthma. *Eur Respir J*, 31, 43-6.

76. <http://www.abcam.com/index.html?pageconfig=resource&rid=10723&pid=10628>